Metallocenes as Reaction Intermediates

By Peter Grebenik
CHEMISTRY UNIT, SCHOOL OF BIOLOGICAL AND MOLECULAR SCIENCES, OXFORD POLYTECHNIC, OXFORD OX3 0BP
Roger Grinter
SCHOOL OF CHEMICAL SCIENCES, UNIVERSITY OF EAST ANGLIA, NORWICH NR4 7TJ
and
Robin N. Perutz
DEPARTMENT OF CHEMISTRY, UNIVERSITY OF YORK, YORK YO1 5DD

1 Introduction

The mechanistic era of chemistry has seen the replacement of the lasso by a sequence of reaction intermediates. We expect evidence for a mechanism to include stereochemical studies of products and reaction kinetics. Direct detection of reaction intermediates is relatively unusual, although a fuller understanding of the reactions surely requires the determination of the electronic and molecular structure of reaction intermediates, in addition to kinetic measurements of their roles in the reactions. The determination of the electronic and molecular structures of the metal carbonyl intermediates $Cr(CO)_5$, $Fe(CO)_4$, and $Mn(CO)_5$ was achieved by matrix isolation methods between 1970 and 1983.[1-3] In the past few years the improvement in fast reaction methods, especially in time-resolved infrared spectroscopy, has led to experimental proof that these molecules do participate in the reactions.[2,4,5] It is now possible to measure the rates of their reactions with substrates directly and to demonstrate that their molecular structures are barely affected by the change of phase from matrix to solution to gas.[2,4] It is no coincidence that these intermediates are nearly always generated by photochemical methods, since photolysis provides one of the most convenient routes to reactive matrix-isolated intermediates and to the study of fast reactions. The success with metal carbonyl intermediates depends on the high infrared intensity and sensitivity to structure of the CO-stretching modes.

[1] R. N. Perutz and J. J. Turner, *Inorg. Chem.*, 1975, **14**, 262; *J. Am. Chem. Soc.*, 1975, **97**, 4791; J. K. Burdett, J. M. Grzybowski, R. N. Perutz, M. Poliakoff, J. J. Turner, and R. F. Turner, *Inorg. Chem.*, 1978, **17**, 147.
[2] M. Poliakoff and E. Weitz, *Acc. Chem. Res.*, 1987, **20**, 408 and references therein.
[3] S. P. Church, M. Poliakoff, J. A. Timney, and J. J. Turner, *J. Am. Chem. Soc.*, 1981, **103**, 7515; M. C. R. Symons and R. L. Sweany, *Organometallics*, 1982, 1, 834; S. A. Fairhurst, J. R. Morton, R. N. Perutz, and K. F. Preston, *ibid.*, 1984, **3**, 1389.
[4] M. Poliakoff and E. Weitz, *Adv. Organomet. Chem.*, 1986, **25**, 277 and references therein.
[5] W. L. Waltz, O. Hackelberg, L. M. Dorfman, and A. Wojcicki, *J. Am. Chem. Soc.*, 1978, **100**, 7259; R. W. Wegman, R. J. Olsen, D. R. Gard, L. R. Faulkner, and T. L. Brown, *ibid.*, 1981, **103**, 6089; H. Yesaka, T. Kobayashi, K. Yasufuku, and S. Nagakura, *ibid.*, 1983, **105**, 6249; S. P. Church, H. Hermann, F. W. Grevels, and K. Schaffner, *J. Chem. Soc., Chem. Commun.*, 1984, 785.

In this review, we examine the role of another group of reaction intermediates, the 16- and 17-electron metallocenes of the heavy transition elements (*i.e.* Mo, W, Re, Os^+), and show that these molecules have many properties which lend themselves to examination by matrix isolation, even though the ν(CO) modes are absent. We also include discussion of the 16-electron bis(cyclopentadienyl)metal monohydrides and monomethyls of niobium and tantalum. These studies underline the variety of organometallic complexes which are susceptible to photodissociation, and have suggested new photochemical experiments in solution, especially with the decamethyl-metallocene derivatives. The direct measurement of the rates of reaction of these molecules in solution has only just begun.

Metallocenes of the first-row transition elements are stable with valence electron counts from 15 to 20 (Cp_2V to Cp_2Ni, $Cp = \eta^5\text{-}C_5H_5$). Neutral complexes and monocations are readily isolated,[6] and in some cases monoanions have also been formed.[7] Only titanocene remains elusive. Expansion of coordination to form complexes of the type Cp_2MX, Cp_2MX_2, *etc.* is common for vanadium and titanium.[6] Chromocene forms one such complex, Cp_2CrCO, but it is thermally very unstable.[8] When we turn to the second- and third-row metals, we find no stable metallocenes, Cp_2M, with less than 18 valence electrons. Instead coordination expansion to Cp_2MX_n becomes the norm—many of the resulting complexes achieve the 18-electron configuration. Among the wide variety of such compounds, the isoelectronic hydride complexes stand out as prototypes (Scheme 1). Attempts to make heavy metallocenes with less than 18 valence electrons usually give dinuclear products related to the titanocene dimers[9] (Scheme 2) in which the metal has achieved electronic saturation by formation of metal–metal bonds and/or insertion into C–H bonds of a cyclopentadienyl unit.[10–12] (Evidence for the metallocenes of the titanium group may be found in ref. 9.)

Bis(η5-cyclopentadienyl)metal Hydrides

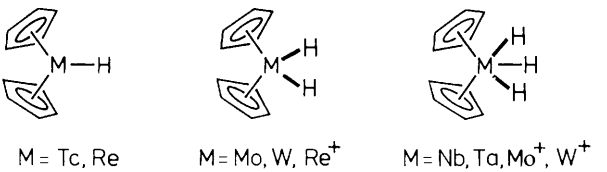

M = Tc, Re M = Mo, W, Re^+ M = Nb, Ta, Mo^+, W^+

Scheme 1

[6] J. P. Collman, L. S. Hegedus, J. R. Norton, and R. G. Finke, 'Principles and Applications of Organotransition Metal Chemistry', University Science Books, New York, 1987

[7] K. Jonas and V. Wiskamp, *Z. Naturforsch.*, 1983, **386**, 1113.

[8] K. L. T. Wong and H. H. Brintzinger, *J. Am. Chem. Soc.*, 1975, **97**, 5143.

[9] G. P. Pez and J. N. Armor, *Adv. Organomet. Chem.*, 1981, **19**, 2; G. E. Toogood and M. G. H. Wallbridge, *Adv. Inorg. Chem. Radiochem.*, 1982, **25**, 267.

Dinuclear Metallocenes

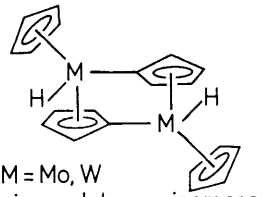

M = Mo, W
cis and trans isomers
$C_{20}H_{20}M_2$

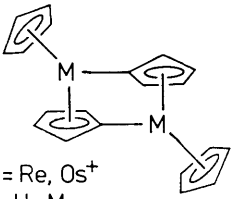

M = Re, Os^+
$C_{20}H_{18}M_2$

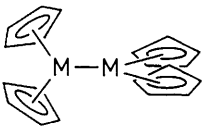

M = Re, Os^+
$C_{20}H_{20}M_2$

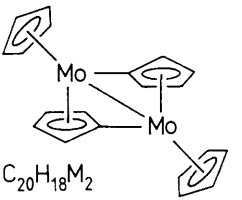

$C_{20}H_{18}M_2$

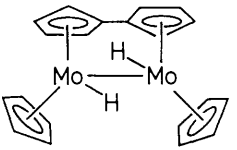

$C_{20}H_{20}M_2$

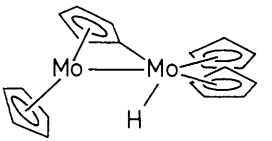

$C_{20}H_{20}M_2$

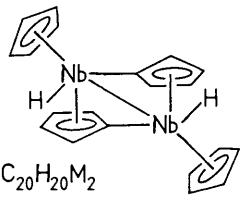

$C_{20}H_{20}M_2$

Scheme 2

[10] M. Berry, N. J. Cooper, M. L. H. Green, and S. J. Simpson, *J. Chem. Soc., Dalton Trans.*, 1980, 29; J. Bashkin, M. L. H. Green, M. L. Poveda, and K. Prout, *ibid.*, 1982, 2485; 2495.

[11] (*a*) L. J. Guggenberger and F. N. Tebbe, *J. Am. Chem. Soc.*, 1971, **93**, 5924; (*b*) P. Pasman and J. J. M. Snel, *J. Organomet. Chem.*, 1984, **276**, 387.

[12] M. M. Droege, W. D. Harman, and H. Taube, *Inorg. Chem.*, 1987, **26**, 1309.

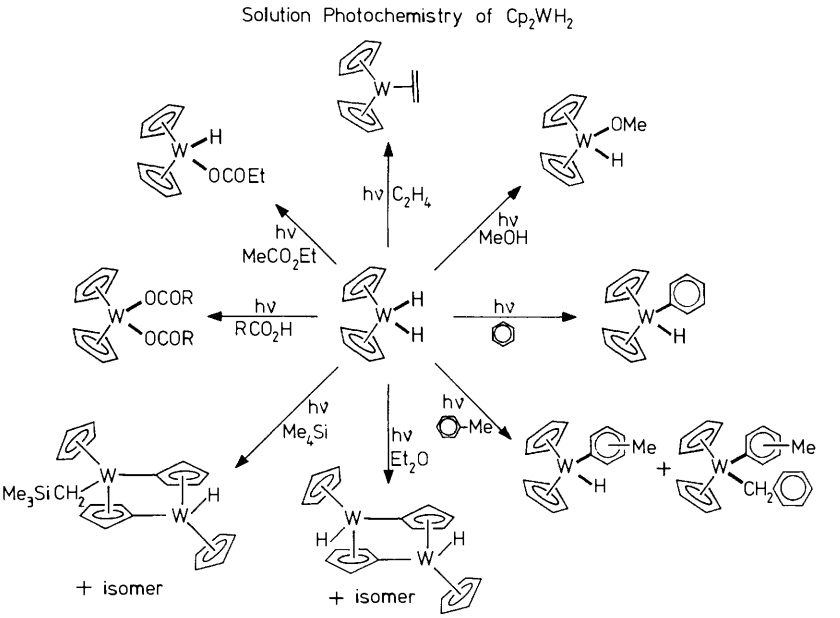

Scheme 3

2 Product Studies in Solution

In 1972 C. Giannotti and M. L. H. Green published the first evidence that photolysis of Cp_2WH_2 in benzene solution generates a tungsten (phenyl) hydride by insertion into a C–H bond of benzene (Scheme 3).[13] Already at this stage they postulated that the reaction proceeded *via* the metallocene intermediate. It soon emerged that photolysis in the presence of a variety of substrates causes reductive elimination of dihydrogen and either direct addition of a new ligand (*e.g.* of CO or C_2H_4) or oxidative addition of a new ligand[14] (with substrates containing O–H, aromatic C–H, or activated sp^3 C–H bonds). The case for a metallocene intermediate in the first stage of oxidative addition was much strengthened by the discovery that almost exactly the same product distribution is obtained by thermal reaction of $Cp_2W(CH_3)H$ with the corresponding substrates.[15] Isotopic labelling confirms that $Cp_2W(CH_3)H$ loses methane in a concerted process provided that it is in dilute solution.[16] Other photochemical sources of Cp_2W include Cp_2WCO and $Cp_2W(C_2H_4)$.[17,18] Tungstenocene will react with a variety

[13] C. Giannotti and M. L. H. Green, *J. Chem. Soc., Chem. Commun.*, 1972, 1114.
[14] M. Berry, K. Elmitt, and M. L. H. Green, *J. Chem. Soc., Dalton Trans.*, 1979, 1950; L. Farrugia and M. L. H. Green, *J. Chem. Soc., Chem. Commun.*, 1975, 416; T. Ho and T. Nakano, *J. Chem. Soc., Dalton Trans.*, 1987, 1857.
[15] N. J. Cooper, M. L. H. Green, and R. Mahtab, *J. Chem. Soc., Dalton Trans.*, 1979, 1557.
[16] R. M. Bullock, C. E. L. Headford, S. E. Kegley, and J. R. Norton, *J. Am. Chem. Soc.*, 1985, **107**, 727.
[17] K. L. T. Wong, J. L. Thomas, and H. H. Brintzinger, *J. Am. Chem. Soc.*, 1974, **96**, 3694.
[18] R. N. Perutz and M. Whittlesey, unpublished.

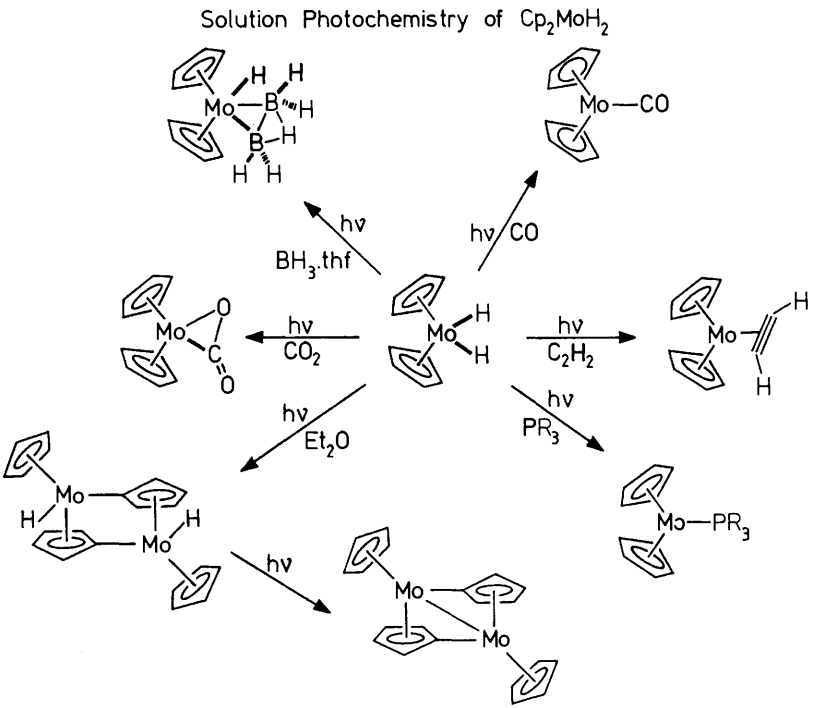

Scheme 4

of C–H bonds of which the least activated are those of tetramethylsilane. In the absence of such a substrate, Cp_2W appears to attack either itself or its precursor to yield dinuclear products of insertion into the C–H bonds of a cyclopentadienyl ring (Scheme 3).[10] These experiments laid the foundations not only for the matrix studies of the unstable metallocenes, but also for the spectacular discoveries of alkane activation by the groups of Bergman, Graham, and Jones.[19–21]

The corresponding experiments on Cp_2MoH_2 showed how different in reactivity from a third-row complex the corresponding second-row complex can be. Although reactive towards 2-electron donor ligands including even CO_2,[22a] molybdenocene does not undergo any oxidative addition reactions with C–H or O–H bonds of added substrates. The only oxidative addition products are a dinuclear complex formed by multiple loss of H_2 and a novel diboranyl-

[19] R. A. Periana and R. G. Bergman, *J. Am. Chem. Soc.*, 1986, **108**, 7332 and references therein.
[20] W. D. Jones and F. J. Feher, *J. Am. Chem. Soc.*, 1982, **104**, 4240; 1985, **107**, 620; 1984, **106**, 1650.
[21] J. K. Hoyano, A. D. McMaster, and W. A. G. Graham, *J. Am. Chem. Soc.*, 1983, **105**, 7190.
[22] (*a*) K. A. Belmore, R. A. Vanderpool, J. C. Tsai, M. A. Khan, and K. N. Nicholas, *J. Am. Chem. Soc.*, 1988, **110**, 2004; (*b*) G. L. Geoffroy and M. G. Bradley, *Inorg. Chem.*, 1978, **17**, 2410; (*c*) P. D. Grebenik, M. L. H. Green, M. A. Kelland, J. B. Leach, P. Mountford, G. Stringer, N. M. Walker, and L. L. Wong, *J. Chem. Soc., Chem. Commun.*, 1988, 799.

(hydride) complex (Scheme 4).[10,22c] The case for concerted loss of dihydrogen from Cp_2MoH_2 is strengthened by the formation of D_2 as the major product of photolysis of Cp_2MoD_2 in C_6H_6.[22b] However, the presence of a significant proportion of HD still leaves some room for doubt. It would be worth repeating this experiment in the presence of added ligand to prevent secondary photolysis. The carbonyl Cp_2MoCO and the oxo complex Cp_2MoO can function as alternative sources of molybdenocene.[17,23] In the latter case, reaction with oxygen leads to formation of $[Cp_2Mo(MoO_4)]_2$ in addition to the more usual products. Evidence for molybdenocene polymers can also be obtained by reduction of Cp_2MoCl_2.

The photochemical reactivity of Cp_2MH_2 (M = Mo, W) depends on the long-wavelength tail in the absorption spectra of these compounds which extends into the visible region beyond the region of substrate absorption, giving them their yellow colour. The quantum yields for photosubstitution of the dihydrides are 0.1 (Cp_2MoH_2) and 0.01 (Cp_2WH_2).[22b] It is thought that photolysis populates directly or indirectly M–(H_2) anti-bonding orbitals (see p. 482). Complexes in the +II oxidation states, such as the carbonyl and ethene complex also have the necessary absorption characteristics for convenient photochemistry, but the M^{VI} complex such as $[Cp_2WH_3]^+$ are white and are photostable.

Photochemical studies of halide and alkyl complexes of molybdenum and tungsten have also been reported but they react by different pathways from the dihydrides, carbonyl, and ethene complexes.[24] Both Cp_2MX_2 and $[Cp_2MX_2]^+$ (X = Cl, Br, I) undergo reaction to $[Cp_2M(X)L]^+$ and $[Cp_2ML_2]^{2+}$ in the presence of L = MeCN. It is thought that the first stage of these reactions involves charge-transfer excitation to form a common radical pair intermediate, $Cp_2MX\cdots X\cdot$. The quantum yield for disappearance of $[Cp_2MCl_2]^+$ is remarkably high, 0.4. The dialkyls Cp_2MMe_2 are photostable, but the corresponding cations $[Cp_2MMe_2]^+$ are photosensitive;[24] the molybdenum complex gives products of the type $[Cp_2M(Me)L]^+$ (L = pyridine, MeCN), while the tungsten complex gives the characteristic products of α-elimination from a $[Cp_2WMe]^+$ intermediate (see ref. 70).

When we move to complexes of the neighbouring elements, absorption spectra suitable for near ultraviolet photochemical reactions in solution are found for Cp_2ReH and for $Cp_2MH(L)$ (M = Nb, Ta; L = CO) but not for the trihydrides Cp_2MH_3 (M = Nb, Ta).[25,26] On the other hand, the latter complexes are much more prone to thermal reaction *via* H_2 loss.

Studies of Cp_2ReH have been hampered by synthetic problems. In the presence of CO, Cp_2ReH reacts both photochemically and thermally to form the η^2-cyclopentadiene complex (equation 1):[25]

[23] N. D. Silavwe, M. R. Bruce, C. E. Philbin, and D. R. Tyler, *Inorg. Chem.*, 1988, **27**, 4669.
[24] S. M. B. Costa, A. R. Dias, and J. S. Pina, *J. Organomet. Chem.*, 1979, **175**, 193; M. J. Calhorda, S. M. B. Costa, A. R. Dias, and F. J. S. Pina, *Nouv. J. Chim.*, 1984, **8**, 619; S. M. B. Costa, A. R. Dias, and F. J. S. Pina, *J. Chem. Soc., Dalton Trans.*, 1981, 314.
[25] J. Chetwynd-Talbot, P. Grebenik, R. N. Perutz, and M. H. A. Powell, *Inorg. Chem.*, 1983, **22**, 1675.
[26] R. F. G. Baynham, J. Chetwynd-Talbot, P. Grebenik, R. N. Perutz, and M. H. A. Powell, *J. Organomet. Chem.*, 1985, **284**, 229.

$$Cp_2ReH \xrightarrow[\text{or } \Delta]{h\nu, CO} Cp(\eta^2\text{-}C_5H_5)Re(CO)_2 \xrightarrow{h\nu, CO} CpRe(CO)_3 + C_5H_6 \qquad (1)$$

Related intramolecular hydrogen-transfer reactions of $CpRe(PR_3)_2H_2$ between ring and metal have been documented in far more detail by Jones and Maguire.[27] No evidence for the homolysis of the Re–H bond of Cp_2ReH in solution has been reported, but preliminary experiments suggest that further photochemical reactions of Cp_2ReH await discovery. Oxidation of $[Cp_2ReLi]_n$ gives rise, probably *via* rhenocene to the rhenocene dimer in which the Re atoms are linked by a metal–metal bond (Scheme 2).[11b]

In a pioneering series of investigations Tebbe and Parshall showed that the trihydrides Cp_2MH_3 (M = Nb, Ta) catalyse H/D exchange between D_2 and aromatics at 80—110 °C, and proposed a mechanism involving insertion into monohydride intermediates.[28] The niobium complex also catalyses exchange between C_6D_6 and Et_3SiH.[29a] (*NB* It now seems possible that Cp_2NbH_3 and $Cp_2NbH(\eta^2\text{-}H_2)$ or even $Cp_2Nb(\eta^3\text{-}H_3)$ are in equilibrium in solution—see p. 478.[29]) A variety of other compounds including $Cp_2MH(L)$ (L = CO, PR_3, C_2H_4, carbene) and $Cp_2Nb(\eta^2\text{-}BH_4)$ can also function as thermal sources of Cp_2MH (M = Nb, Ta).[28,30] Thermal reaction of Cp_2NbH_3 in the absence of substrate gives the dimer shown in Scheme 2.[11] Photochemical investigations of Cp_2MH_3 and $Cp_2M(H)CO$ (M = Nb, Ta) in solution are more restricted. The carbonyl complexes react with H_2 to form the trihydrides and with PEt_3 to give $Cp_2MH(PEt_3)$ on irradiation.[31] The trihydrides themselves undergo photo-induced replacement of H_2 by CO or PEt_3 in toluene solution and photolytic H/D exchange with C_6D_6.[31] It is not yet established that the reactions of the trihydrides involve direct absorption, since it seems unlikely that they absorb beyond the cut-off of the arene. Nevertheless, all these reactions were postulated to proceed *via* Cp_2MH intermediates. The photochemical reactions of the trihydrides with $CpNb(CO)_4$, $Mn_2(CO)_{10}$, MeSSMe and Bu^tOOBu^t almost certainly involve excited states of these highly photosensitive substrates rather than of the trihydrides themselves.[32]

Photolysis of the group V dialkyls, Cp_2MMe_2 appears to cause homolysis of a metal–methyl bond.[33] When M = Ta, the organic products include methane and

[27] W. D. Jones and J. A. Maguire, *Organometallics*, 1987, **6**, 1301.

[28] E. K. Barefield, G. W. Parshall, and F. N. Tebbe, *J. Am. Chem. Soc.*, 1970, **92**, 5234; F. N. Tebbe and G. W. Parshall, *ibid.*, 1971, **93**, 3793; U. Klabunde and G. W. Parshall, *ibid.*, 1972, **94**, 9087.

[29] M. D. Curtis, L. G. Bell, and W. M. Butler, *Organometallics*, 1985, **4**, 701; J. F. Reynoud, J.-C. Leblanc, and C. Moise, *Transition Met. Chem.*, 1985, **10**, 291; A. Antinolo, B. Chaudret, G. Commenges, M. Fajardo, F. Jalon, R. H. Morris, A. Otero, and C. T. Schweitzer, *J. Chem. Soc., Chem. Commun.*, 1988, 1210.

[30] A. A. Pasynskii, Yu. V. Skripkin, V. T. Kalinnikov, M. A. Porai-Koshits, A. S. Antskyshkina, G. G. Sadikov, and V. N. Ostrikova, *J. Organomet. Chem.*, 1980, **201**, 269; R. S. Threlkel and J. E. Bercaw, *J. Am. Chem. Soc.*, 1981, **103**, 2650.

[31] D. F. Foust, R. D. Rogers, M. D. Rausch, and J. L. Atwood, *J. Am. Chem. Soc.*, 1982, **104**, 5646.

[32] W. A. Hermann, H. Biersack, M. L. Ziegler, and P. Wülknitz, *Angew. Chem., Int. Ed. Engl.*, 1981, **20**, 388; S. Baral, J. A. Labinger, W. R. Scheidt, and F. J. Timmers, *J. Organomet. Chem.*, 1981, **215**, C55; F. J. Timmers, W. R. Scheidt, J. A. Labinger, and S. Baral, *ibid.*, 1982, **240**, 153; J. L. LeQuere, F. Y. Petillon, J. E. Guerchais, and J. Sala-Pala, *Inorg. Chim. Acta*, 1980, **43**, 5.

[33] D. F. Foust and M. D. Rausch, *J. Organomet. Chem.*, 1982, **226**, 47; D. F. Foust, M. D. Rausch, and E. Samuel, *ibid.*, 1980, **193**, 209.

cyclopentadiene, while the organometallic intermediate, probably Cp_2TaMe, undergoes disproportionation to tantalocene polymer and Cp_2TaMe_3. In the presence of CO, the intermediate is trapped as $Cp_2TaMe(CO)$.[33] Evidence for Cp_2TaMe as an intermediate is also obtained on photolysis of $Cp_2Ta(C_2H_4)Me$, which effects replacement of the ethene ligand.[34] However, Cp_2TaMe may be in equilibrium with $Cp_2Ta(H)(CH_2)$ like Cp^*_2TaMe ($Cp^* = \eta^5$-C_5Me_5) and $[Cp_2WMe]^+$ (see p. 488).

The reactions described above are postulated to proceed *via* Cp_2MX (X = H, Me) intermediates, rather than simple metallocenes. However, there is good evidence from e.p.r. spectra in solution that Cp_2Nb is formed on reduction of Cp_2NbCl_2 with sodium naphthalide and other reductants. The e.p.r. signal shows coupling to ^{93}Nb and disappears by second-order kinetics. The final product is the dimer shown in Scheme 2.[35]

3 Electronic Structure of Metallocenes

There is ample evidence from many spectroscopic methods that the electronic structure of all known transition-metal sandwich complexes is excellently described by a ligand-field model. The case for the use of this model has been put most ably by Warren[36] and by Green[37] but unfortunately it has been obscured by some misleading molecular orbital calculations which have been cited all too frequently.[38] According to the ligand-field model (Figure 1), the *d* orbitals split into three sets: the e_2 set is most tightly bound and is capable of interacting with vacant ligand π^* orbitals, the a_1 orbital is only weakly involved in bonding because the ligand a_1 combination lies so deep. The e_1 set is antibonding through interaction with the occupied ligand π set of the same symmetry. (We use symbols appropriate to D_5 symmetry in most parts of this review, since this does not prejudge the orientation of the rings, but in some examples we revert to D_{5d} symmetry to highlight the effect of the centre of symmetry.) The e_2 pair carry two units of orbital angular momentum, the e_1 pair one unit. This diagram can be applied equally well to $(arene)_2M$ complexes with D_6 symmetry.

With a d^4 metal, three different electronic ground configurations (and states) arise excluding the high-spin arrangement. These configurations and the resulting electronic states are shown in Figure 2a. The diamagnetic $^1A_1$ state is found for the ground state of bz_2Ti (bz = η^6-C_6H_6), while the $^3E_2$ state is found for chromocene.[36,37] The $^3A_2$ state is unknown. The $^3E_2$ state is subject to either or both of Jahn–Teller distortion and spin–orbit coupling. With one unit of spin and two of orbital angular momentum, three spin–orbit sub-states are formed (Figure 2b). The lowest energy state has E_2 symmetry and three units of angular

[34] P. R. Sharp and R. R. Schrock, *J. Organomet. Chem.*, 1979, **171**, 43.

[35] D. A. Lemenovskii and V. P. Fedin, *J. Organomet. Chem.*, 1977, **132**, C11; A. N. Nesmeyanov, D. A. Lemenovskii, V. P. Fedin, and E. G. Perevalova, *Dokl. Akad. Nauk SSSR*, 1979, **245**, 609.

[36] K. D. Warren, *Struct. Bonding (Berlin)*, 1976, **27**, 45.

[37] (*a*) J. C. Green, *Struct. Bonding (Berlin)*, 1981, **43**, 37; (*b*) J. C. Green, cited in ref. 67.

[38] A. Haaland, *Acc. Chem. Res.*, 1979, **12**, 415; A. W. Parkins and R. C. Poller, 'An Introduction to Organometallic Chemistry', MacMillan, London, 1986; F. A. Cotton and G. Wilkinson, 'Advanced Inorganic Chemistry', 4th Edition, Wiley, New York, 1980.

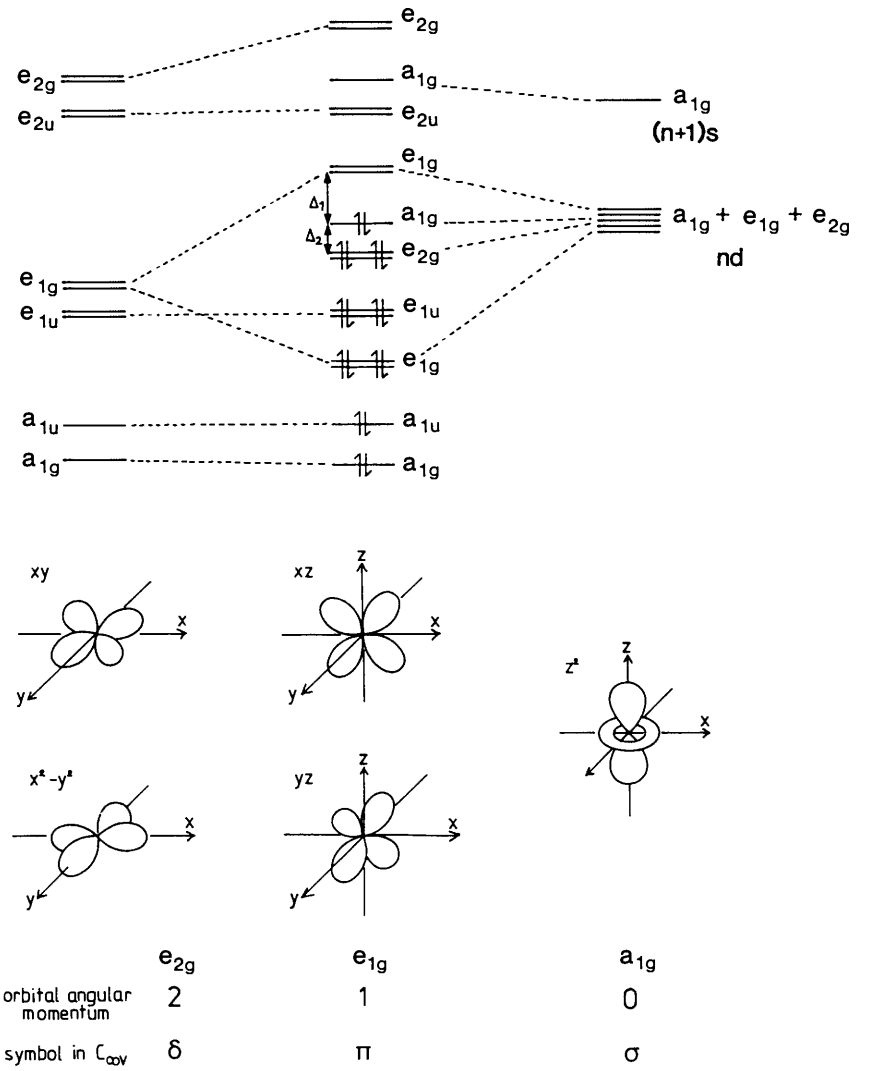

Figure 1 *Above: Molecular orbital interaction diagram for a metallocene in* D_{5d} *symmetry. The orbitals are filled up to the level for an* 18 *electron complex. In* D_5 *symmetry the subscripts are dropped; in* D_{5h} *symmetry, the* g *and* u *symbols are replaced by prime and double primes respectively* (Adapted with permission from Green, *Struct. Bonding. (Berlin)*, 1981, **43**, 37, ref. 37*a*)

Below: The form of the d *orbitals contributing to the* e_{2g}, e_{1g}, *and* a_{1g} *frontier orbitals, their contribution to the orbital angular momentum, and their analogues in the closely-related* $C_{\infty v}$ *point group*

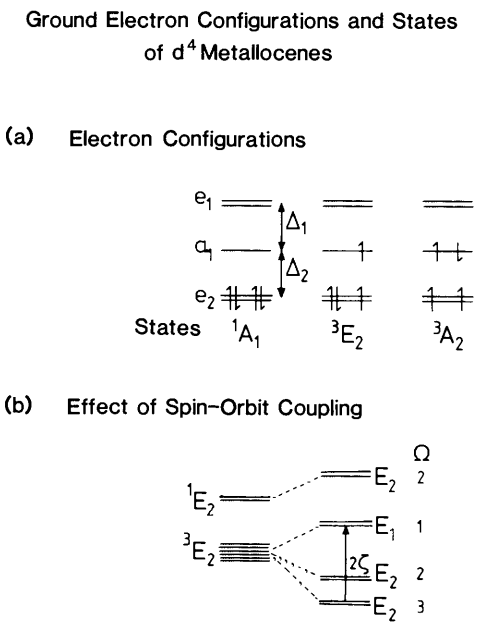

Figure 2 *(a) The ground electron configurations possible for a* d^4 *metallocene and the corresponding electronic states. Only the* $^3E_2$ *state has been observed for metallocenes, but the* $^1A_1$ *state is found for bis(arene) compounds. (b) The effect of spin–orbit coupling on the* $^3E_2$ *state and the corresponding singlet. The arrow shows the vibronic transition between the spin–orbit sub-states observed for* Cp_2W. *The symbol* Ω *shows the total angular momentum quantum number in* $C_{\infty v}$ *symmetry*

momentum ($\Omega = 3$). In the presence of a magnetic field perpendicular to the molecular axis, this state does not split ($g_\perp = 0$) unless there is a distortion. In a parallel field it splits into two levels separated by $2g_\parallel \mu_B B$. In the absence of covalent delocalization $g_\parallel$ takes the value of 4. The g values can be related to the magnetic moments provided that only one Kramers' doublet is populated:

$$\mu_\parallel{}^2 = 0.75\, g_\parallel{}^2 \qquad \mu_\perp{}^2 = 0.75\, g_\perp{}^2$$
$$\langle \mu^2 \rangle = 1/3\,(\mu_\parallel{}^2 + 2\mu_\perp{}^2) \tag{2}$$

A sandwich complex with five d electrons can adopt one of three different ground state configurations (Figure 3a), a high-spin state and two low-spin configurations one with an a_1 vacancy, the other with an e_2 vacancy. The $^2A_1$ state is not adopted by metallocenes, but is found for all d^5 $(arene)_2M$.[36,37,39,40]

[39] F. G. N. Cloke, A. N. Dix, J. C. Green, R. N. Perutz, and E. A. Seddon, *Organometallics*, 1983, **2** 1150; J. A. Bandy, A. Berry, M. L. H. Green, R. N. Perutz, K. Prout, and J. N. Verpaux, *J. Chem. Soc., Chem. Commun.*, 1984, 729.

[40] M. P. Andrews, S. B. Mattar, and G. A. Ozin, *J. Phys. Chem.*, 1986, **90**, 1037.

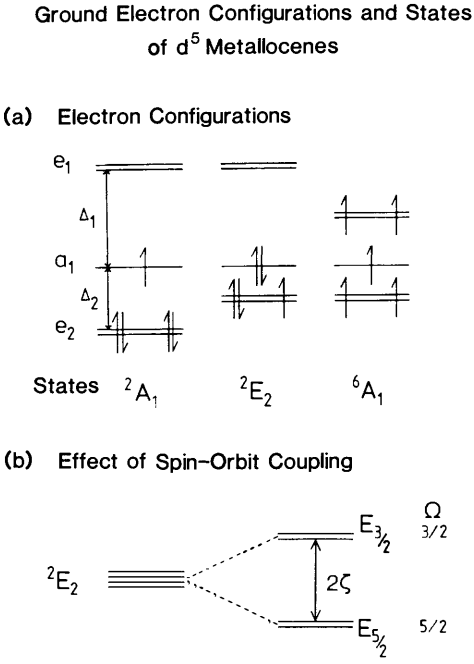

Figure 3 (*a*) *The ground electron configurations possible for a* d^5 *metallocene and the corresponding states. The* $^2E_2$ *state is found for heavy metallocenes.* (*b*) *The effect of spin–orbit coupling on the* $^2E_2$ *state. The symbol* Ω *shows the total angular momentum quantum number*

Characteristically, it has both $g_{\|}$ and $g_{\perp}$ very close to 2, since there is no orbital angular momentum. The $^2E_2$ state is adopted by $[Cp_2Fe]^+$, $[Cp^*_2Fe]^+$, and by Cp^*_2Mn.[41] It is related to the $^3E_2$ state of the d^4 systems by addition of an a_1 electron, so it behaves very similarly and it is subject to both Jahn–Teller and spin–orbit effects. Two spin–orbit sub-states are formed, $E_{5/2}$ ($\Omega = 5/2$) and $E_{3/2}$ ($\Omega = 3/2$) (Figure 3b, these term symbols correspond to irreducible representations of the double group, D_5*). Manganocene and substituted complexes $(\eta^5\text{-}C_5H_4R)_2Mn$ either may be switched between $^2E_2$ and $^6A_1$ states by a change of host material, or exhibit an equilibrium between them.[37,42,43] The effect of both dynamic and static Jahn–Teller distortions can be seen in the e.p.r. spectra of manganocenes.[42] In the current review, the electronic structure of $[Cp_2Os]^+$ is of

[41] D. M. Duggan and D. N. Hendrickson, *Inorg. Chem.*, 1975, **14**, 955; J. L. Robbins, N. M. Edelstein, S. R. Cooper, and J. C. Smart, *J. Am. Chem. Soc.*, 1979, **101**, 3853.

[42] J. H. Ammeter, *J. Magn. Reson.*, 1978, **30**, 229; J. H. Ammeter, B. Bucher, and N. Oswald, *J. Am. Chem. Soc.*, 1974, **96**, 7833; J. H. Ammeter, N. Oswald, and R. Bucher, *Helv. Chim. Acta*, 1975, **58**, 671; J. H. Ammeter, L. Zoller, J. Bachmann, P. Baltzer, E. Gamp, R. Bucher, and E. Deiss, *ibid.*, 1981, **64**, 1063.

[43] N. Hebendanz, F. H. Köhler, G. Müller, and J. Riede, *J. Am. Chem. Soc.*, 1986, **108**, 3281; D. Cozak and F. Gauvin, *Organometallics*, 1987, **6**, 1912.

particular interest. Photoelectron spectra of Cp_2Os show that the ground state of the corresponding cation is $E_{5/2}$ with the $^2A_1$ state lying 0.41 eV above it.[37b]

The need to examine the detailed workings of spin–orbit coupling and Jahn–Teller effects and the requirement to predict signs of magnetic circular dichroism has necessitated a more thorough analysis than that available through conventional use of group theory. Warren approached this type of problem using the $C_{\infty v}$ point group which is closely related to D_5, but this method gives rise to a prolonged sequence of representations (Σ, Π, Δ, Γ ...) and so misses the cyclic relationship between A_1, E_1, and E_2 characteristic of fivefold or sixfold symmetry. In our analysis, we employed an elegant method developed by P. A. Cox which starts by considering the effect of $\hat{C}_5$ and $\hat{\sigma}_d$ operators on complex orbital functions in D_{5d} symmetry. We need to consider the individual complex components such as $|E_{2g'}\rangle$ and $|E_{2g^-}\rangle$ because they are affected differently by the magnetic field or the Jahn–Teller operator.[46]

$$\begin{aligned} \hat{C}_5|E_{2g\pm}\rangle &= e^{\pm 4\pi i/5}|E_{2g\pm}\rangle \\ \hat{C}_5|E_{1g\pm}\rangle &= e^{\pm 2\pi i/5}|E_{1g\pm}\rangle \end{aligned} \tag{3}$$

The next stage is to pick out the operator and matrix elements appropriate to the problem (examples are given for an E_{2g} ground state):

Jahn–Teller $\langle E_{2g\pm}|H_{JT\pm}|E_{2g\pm}\rangle$ (4)

Ground-state magnetic moment $\langle E_{2g\pm}|\mu_\pm|E_{2g\pm}\rangle$ (5a)
and $\langle E_{2g\pm}|\mu_0|E_{2g\pm}\rangle$ (5b)

Electric dipole transition $\langle E_{2g\pm}|m_\pm|E_{2u\pm}\rangle$ (6a)
and $\langle E_{2g\pm}|m_0|E_{2u\pm}\rangle$ (6b)

As usual we need to examine whether such matrix elements are non-zero. This can be achieved by applying the $\hat{C}_5$ operator to each component of the matrix element. For instance, when we consider the element (6a) needed for absorption/m.c.d., we label any member of the complex pairs ρ, σ, τ, for $E_{2g\pm}$, $m_\pm$, and $E_{2u\pm}$ respectively where ρ, σ, and τ can take the values ± 1. Remembering the sign reversal for the complex conjugate we find that:

$$\hat{C}_5\langle E_{2g\rho}|m_\sigma|E_{2u\tau}\rangle = e^{2\pi i x/5}\langle E_{2g\rho}|m_\sigma|E_{2u\tau}\rangle$$

where $x = -2\rho + \sigma + 2\tau$. The matrix element will be non-zero if $x = 0$ (impossible to satisfy) or if $x = \pm 5$. This latter condition reflects the cyclic nature of the point group and can be satisfied if $\rho = 1$, $\sigma = -1$, $\tau = -1$ or if $\rho = -1$, $\sigma = 1$, $\tau = 1$. There are therefore two non-zero matrix elements of this type:

$$\langle E_{2g+}|m_-|E_{2u-}\rangle \text{ and } \langle E_{2g-}|m_+|E_{2u+}\rangle$$

Examples of the selection rules derived by this method for magnetic circular dichroism are illustrated below (see Figure 10).

4 Photochemical Matrix Isolation

The principles of photochemical matrix isolation experiments are shown in

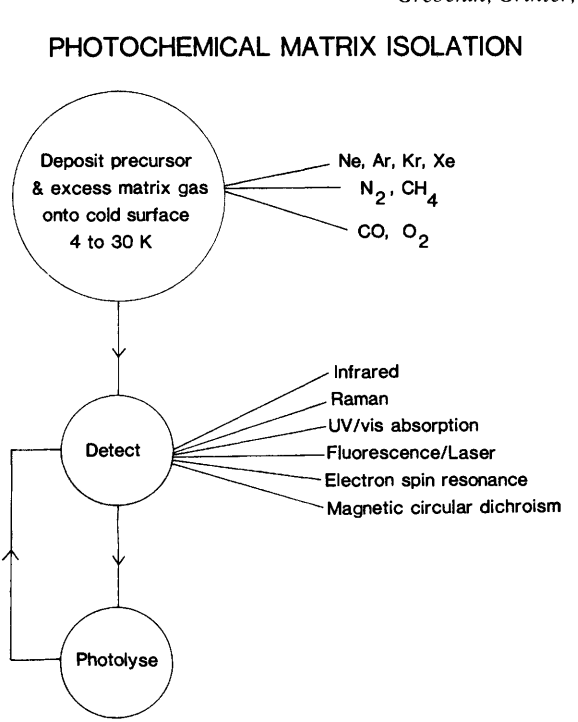

Figure 4 *Schematic diagram showing the principles of photochemical matrix isolation involving the stages of deposition, detection, and photolysis. The matrix materials and the principal detection methods are shown at the right*

Figure 4.[44] The vapour of an organometallic precursor, *e.g.* Cp_2WH_2, is deposited together with a large excess of matrix gas onto a transparent window held at 4—20 K. The matrix gas may be inert (*e.g.* Ar) or more reactive (*e.g.* CO, N_2, CH_4). The unstable photoproduct is generated by *in situ* photolysis. Precursor and photoproducts may be detected by a wide variety of spectroscopic methods (Figure 4): i.r., u.v./vis absorption, laser-induced fluorescence (l.i.f.) and magnetic circular dichroism (m.c.d.) have been employed on the unstable metallocenes. Two limitations of the technique may be observed at this stage: (i) the precursor must be capable of being vaporized without too much decomposition, (ii) the photochemical generation of products may be hampered or prevented by in-cage recombination even at these low temperatures (the cage effect). In practice, the first limitation provides few obstacles to the investigation of neutral complexes, but the second hampers studies of some photoprocesses, especially homolytic cleavage, *e.g.* of a metal–alkyl bond. The matrix material presents no barrier to molecular rearrangement in the adiabatic limit. It follows

[44] R. N. Perutz, *Annu. Rep. Prog. Chem., Section C*, 1985, **82**, 157.

that it stabilizes reaction intermediates in their *ground electronic states with the same molecular structure as in fluid phases.* Excited states are not stabilized; indeed their lifetimes are usually shorter than in the gas phase. It is also well-established that the matrix exercises only a minor solvent effect on most spectroscopic parameters. Nevertheless, specific interactions can take place, as have been documented for $Cr(CO)_5$.[1] Spectra are usually far sharper than those observed in solution or solid phases, because of the quenching of rotation and the low temperature. Provided that the matrix is sufficiently dilute, the proportion of neighbouring precursor molecules in the matrix is negligible, and bimolecular reactions between photoproduct and precursor, or between two photoproducts are prevented. By doping the matrix with other gases (*e.g.* CO) bimolecular reaction with the dopant may occur. However, the spectra in such mixed matrices are usually much broader than in pure ones because of the inhomogeneous environment.

A. Magnetic Circular Dichroism.—Two of the methods of detection, m.c.d. and l.i.f., are less familiar. When a magnetic field lifts the degeneracy of a Kramers' doublet, the levels are split by an energy $Ng\mu_B B$ where N is the number of unpaired electrons. Whereas e.p.r. probes transitions between these levels, circularly polarized light selects transitions from either of these levels to an upper electronic state. Transitions from one level are allowed with left-circularly polarized (LCP) light, transitions with right-circularly polarized (RCP) light proceed from the other level (Figure 5).[45] M.c.d. spectra probe the difference in absorbance between LCP and RCP light; the effect depends on the population differences of the two levels (the C term). The population of the lower level will increase as the temperature falls or the magnetic field increases. Proof of paramagnetism may be established simply by the observation of an m.c.d. signal which increases in intensity as the temperature falls, but it is possible to take the observations a stage further and to determine the g values too. Initially, we used a method of band areas in which we compared the integrated absorbance with the integrated dichroism.[46] This method proved to be error-prone, because of the difficulties of determining meaningful band areas using two different spectrometers on the same sample. More recently, we have determined g values by fitting the magnetization curve.[47] Here we measure the m.c.d. signal as function of the magnetic field and measure the temperature very accurately at the same time. We have used a specially built cryostat for this purpose which allows measurements to be made up to 10 T at 1.5 K (Figure 6).[48] At these temperatures and fields, the Zeeman splitting exceeds kT so that the entire population may be in the lowest Zeeman state and magnetization is complete (see Figure 9). We have demonstrated using samples of tol_2V and Cp^*_2Re (tol = η^6-toluene) with known g

[45] S. B. Piepho and P. N. Schatz, Group Theory in Spectroscopy with Applications to Magnetic Circular Dichroism, Wiley, New York, 1983.
[46] P. A. Cox, P. Grebenik, R. N. Perutz, M. D. Robinson, R. Grinter, and D. R. Stern, *Inorg. Chem.*, 1983, **22**, 3614.
[47] R. G. Graham, R. Grinter, and R. N. Perutz, *J. Am. Chem. Soc.*, 1988, **110**, 7036.
[48] R. G. Graham, R. Grinter, D. R. Stern, and K. Timms, *J. Phys. E*, 1986, **19**, 776.

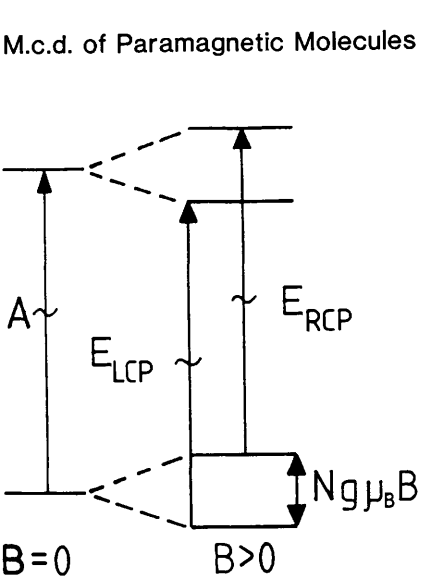

Figure 5 *Schematic energy level diagram showing the relation of absorption to magnetic circular dichroism (m.c.d.) of paramagnetic molecules* (C *term*). *At left normal absorption occurs in the absence of a magnetic field. At right these levels are split by a magnetic field,* B, *parallel to the direction of light propagation into two Zeeman sub-levels separated by* $Ng\mu_B B$ *for a system with* N *unpaired electrons. Transitions from the lower member of the Zeeman doublet are permitted only with left-circularly polarized* (LCP) *light, from the upper member of the pair only with right-circularly polarized* (RCP) *light. The intensity of the resulting dichroism depends on the relative populations of the two Zeeman sub-levels*

values that this method allows the accurate determination of g values.[47,49] M.c.d. spectroscopy is particularly effective for the investigation of paramagnetism of the metallocenes because (a) the magnetic effects are optically determined, so it establishes directly that the same species causes the optical absorption as that exhibiting the magnetic effect (contrast e.p.r.); (b) the method is applicable to systems with even numbers of unpaired electrons or with high orbital angular momenta. In contrast, e.p.r. spectra may not be observable in such circumstances because of zero-field splittings, short relaxation times, and selection rules preventing observation of molecules with $g_\perp = 0$.

B Laser-induced Fluorescence.—Laser-induced fluorescence is a method which can be used to probe the same electronic transitions in emission as those observed in absorption. Whereas absorption spectra show structure corresponding to the vibrational levels of the electronically excited state, the structure in emission spectra corresponds to ground state vibrations.[50] When the transition is

[49] J. A. Bandy, F. G. N. Cloke, G. Cooper, J. P. Day, R. G. Graham, R. B. Girling, J. C. Green, R. Grinter, and R. N. Perutz, *J. Am. Chem. Soc.*, 1988, **110**, 5039.
[50] R. N. Perutz, *Chem. Rev.*, 1985, **85**, 97.

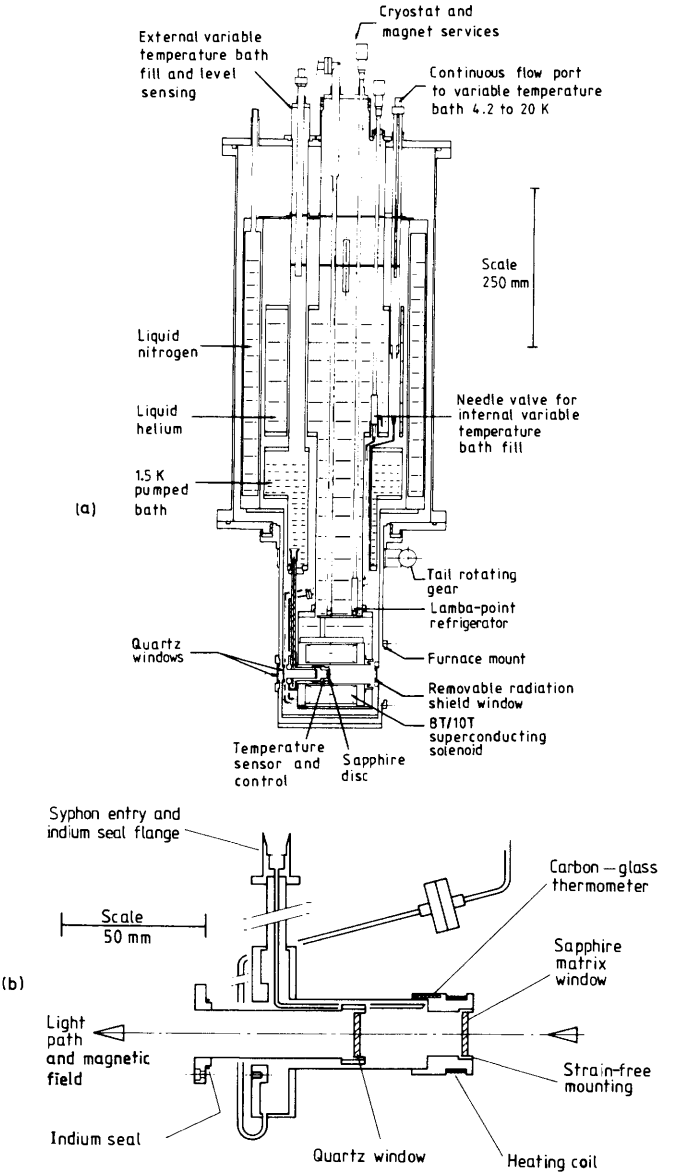

Figure 6 *Diagram of the cryostat employed for magnetization studies via m.c.d. at temperatures down to* 1.5 K *and magnetic fields up to* 10 T. (*a*) *Vertical section through the cryostat.* (*b*) *Enlarged vertical section through the sample area. The sample is deposited on the sapphire matrix window which is in direct contact with the refrigerant*
(Reprinted with permission from Graham *et al., J. Phys. E.*, 1986, **19**, 776, ref. 48)

allowed, the vibrational fine structure usually corresponds to totally symmetric vibrational modes which are forbidden in the infrared. The use of the laser in exciting the emission drastically increases the sensitivity of the method and gives much sharper spectra because of the selectivity of the highly monochromatic laser beam. The experiment may be carried out with a standard Raman spectrometer, but the signal is far more intense than in normal Raman spectroscopy. A fluorescence signal may be distinguished from a resonance Raman spectrum, because its absolute frequency is independent of the frequency of the exciting laser.

5 Generation and Properties of Reactive Metallocenes in Matrices

A. Tungstenocene.[46,47,51]—When an argon matrix containing Cp_2WH_2 is subjected to u.v. photolysis, the i.r. spectrum shows substantial conversion into a new organometallic product. There are several indicators that this product is tungstenocene, Cp_2W: (i) the product spectrum is very similar to the matrix i.r. spectra of ferrocene and vanadocene in the region 3000—500 cm^{-1} (Figure 7); (ii) replacement of the starting material by Cp_2WD_2 has no effect on the product spectrum; (iii) ring deuteriation causes similar shifts in the spectrum to those observed for ferrocene; (iv) the bands in the region below 500 cm^{-1} which correspond to the skeletal vibrations are moved to low frequency compared to ferrocene, as expected for a heavier metal; (v) most importantly, use of alternative precursors Cp_2WL (L = CO, C_2H_4, O) or $Cp_2W(CH_3)H$, gives the same organometallic photoproduct together with characteristic bands of expelled ligands L or CH_4 (Scheme 5). There is one exception to the similarity of the i.r. bands of tungstenocene and those of the stable metallocenes. The strongest band in the i.r. spectrum of Cp_2W is at 3 240 cm^{-1}, is broad by matrix standards and has no counterpart in the stable metallocenes. On ring deuteriation, this band shifts only 15 cm^{-1} proving that it cannot be due to a strange C–H vibration since it should then shift about 1000 cm^{-1}. It was Dr. J. C. Green who first pointed out that it must be an electronic transition, but it was only with the advice of Dr. P. A. Cox that we were able to identify the exact transition (see below).

Are the rings of tungstenocene parallel or do they remain bent as in the precursor? The comparison with the spectra of stable complexes may be taken a stage further by examining the i.r. spectra of pairs of molecules Cp_2M and Cp_2MCO (M = Cr, V, W). Bending of the molecular skeleton introduces a large number of extra i.r. bands, so tungstenocene must have the parallel ring structure.

A further indicator of the structure comes from the u.v./vis spectrum, a method not usually considered to carry structural information. Tungstenocene exhibits an intense absorption in the near ultraviolet, with highly resolved vibrational fine structure (Figure 8). Organometallics rarely show resolved vibrational fine structure because a variety of modes overlap to give broad bands. Exceptions are to be found only in high symmetry situations (*e.g.* $[Cp_2Fe]^+$), where the vibrations are excited very selectively. Thus, this fine structure is a strong indicator of a parallel ring structure. A final piece of evidence for this structure comes from the electronic infrared band (see below). None of these spectroscopic

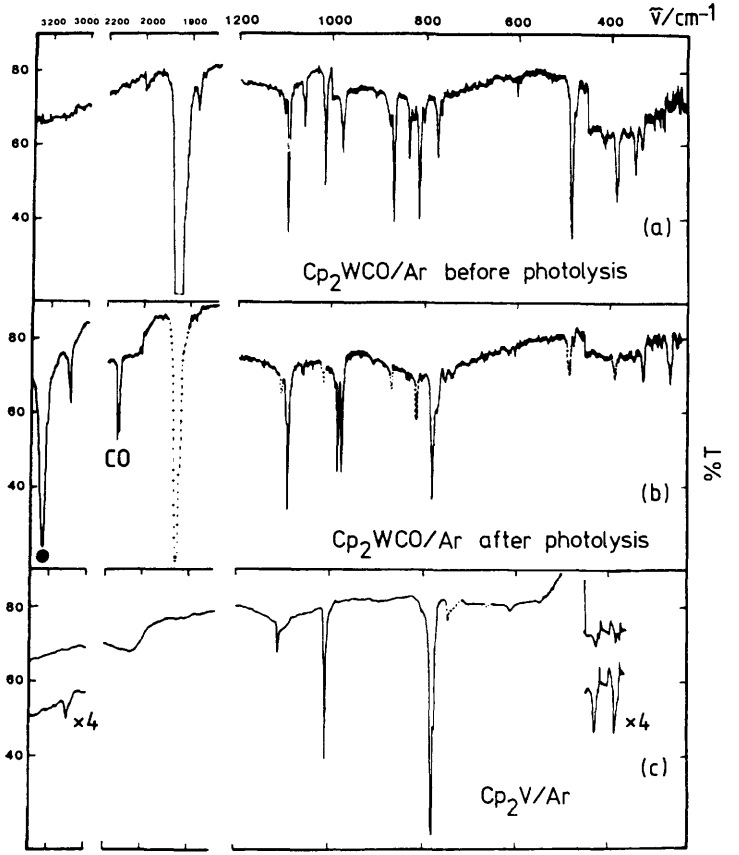

Figure 7 *I.r. spectra illustrating the formation of* Cp_2W. (*a*) *I.r. spectrum of* Cp_2WCO *in an argon matrix at* 10 K *before photolysis,* (*b*) *after* 40 min *u.v. photolysis. The full line shows the product bands, the broken line shows the starting material; notice the electronic transition of* Cp_2W *at* 3240 cm^{-1} (●) *and the band of free* CO. (*c*) *Spectrum of* Cp_2V *in argon shown for comparison*
(Adapted with permission from Grebenik *et al.*, *J. Chem. Soc., Chem. Commun.*, 1979, 742, ref. 51)

methods, on the other hand, offer any useful distinction between different orientations of the rings relative to one another (D_{5h}, D_{5d}, or D_5 symmetry).

The matrix experiments provide only limited opportunities to examine the reactivity of tungstenocene. Photolysis of Cp_2WH_2 in a CO matrix causes production of Cp_2W and Cp_2WCO. This experiment also demonstrates that the elimination of H_2 is concerted, since no HCO is detected (contrast Cp_2ReH p. 476). By using a xenon matrix, it is possible to generate Cp_2W photochemically from the carbonyl and then show that it reacts with CO on warming to about 60 K. It does not react with nitrogen or methane under matrix conditions.

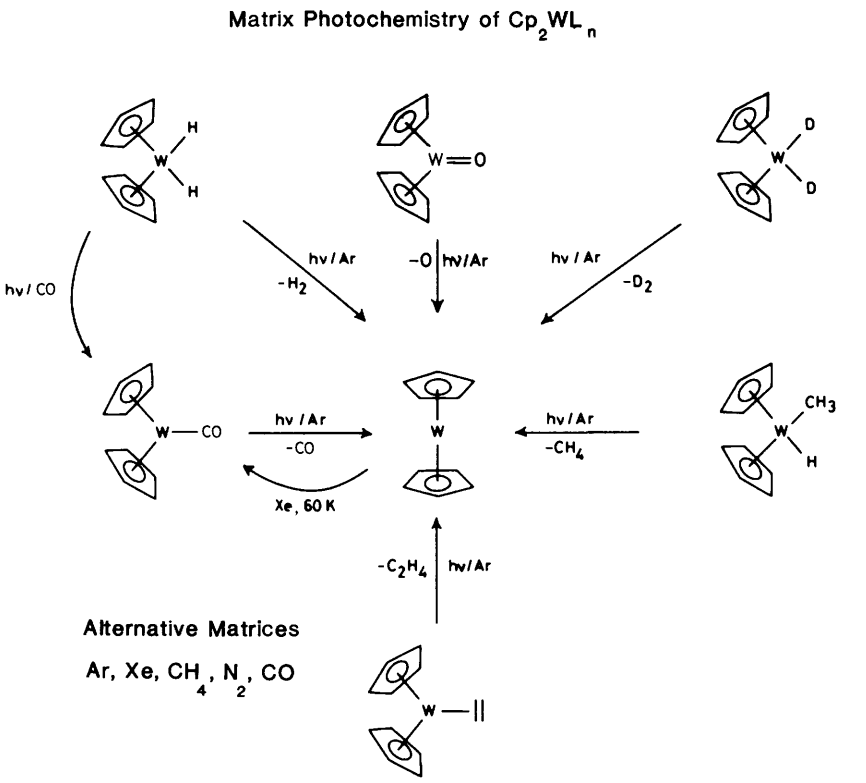

Scheme 5

Is tungstenocene paramagnetic, and if so, which ground state is applicable? As explained on p. 466, the temperature dependence of the m.c.d. spectrum acts as a probe of paramagnetism. The m.c.d. spectrum of Cp_2W closely resembles the absorption spectrum and shows a strong inverse temperature dependence, proving that the molecule is paramagnetic (Figure 8). Analysis of the magnetization curve (Figure 9) monitored at 1.8 and 15 K shows that the molecule has the E_2 ($\Omega = 3$) ground state and gives us a value of $g_{\|} = 3.07 \pm 0.15$. Through this analysis we can explain the electronic infrared band. The intraconfigurational $E_2(\Omega = 3) \rightarrow E_2$ ($\Omega = 1$) transition is vibronically allowed and has an energy of $(2\zeta + \nu)$ where ζ is the spin–orbit coupling constant and ν is the frequency of the allowing mode. We may deduce that $1450 < \zeta < 1570$ cm^{-1} (compare 2580 cm^{-1} for $[Cp_2Os]^+$).[37b] What has happened to the Jahn–Teller distortion? If we compare the i.r. spectra of matrix-isolated ferrocene and chromocene, we see that a Jahn–Teller distortion in chromocene broadens the bands and drastically alters their intensity distribution. The spectrum of tungstenocene corresponds to the

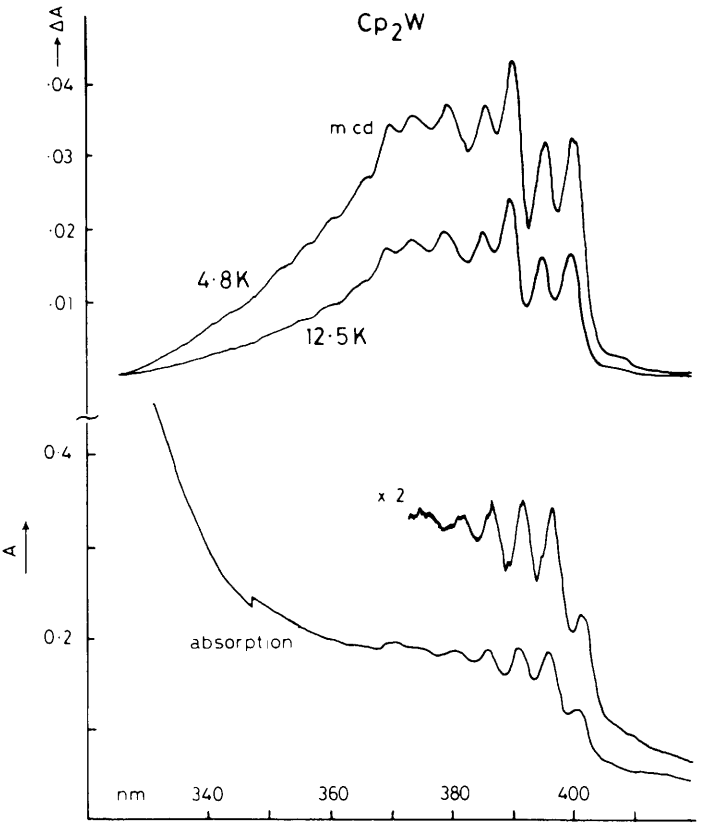

Figure 8 *Below: U.v. absorption spectra of* Cp_2W *at* 12.5 K *obtained following* 30 min *photolysis of* Cp_2WH_2 *in Ar matrix. Above: m.c.d. spectra of the same region measured at a magnetic field of* 1.7 T *on the same sample at* 12.5 K *and after cooling to* 4.8 K. *Notice the increase in m.c.d. intensity on cooling indicative of a paramagnetic ground state. The vibrational progression is associated with the symmetric (ring–metal–ring) stretching mode superimposed on the fully allowed l.m.c.t. transition*
(Reproduced with permission from Cox *et al.*, *Inorg. Chem.*, 1983, **24**, 3614, ref. 46)

undistorted structure, so the Jahn–Teller distortion has been quenched by the spin–orbit coupling. A quantum-mechanical analysis shows that the lowest spin–orbit component is indeed not subject to first-order Jahn–Teller coupling.

The intense low-energy u.v. band of tungstenocene must be a charge-transfer transition. The direction of charge-transfer may be established by making the corresponding compound with C_5H_4Me rings: a shift of 920 cm^{-1} to lower energy proves that it is a ligand-to-metal transition. The analysis of the sign of the m.c.d. by the method described above shows that the upper state has E_2 symmetry (Figure 10a).

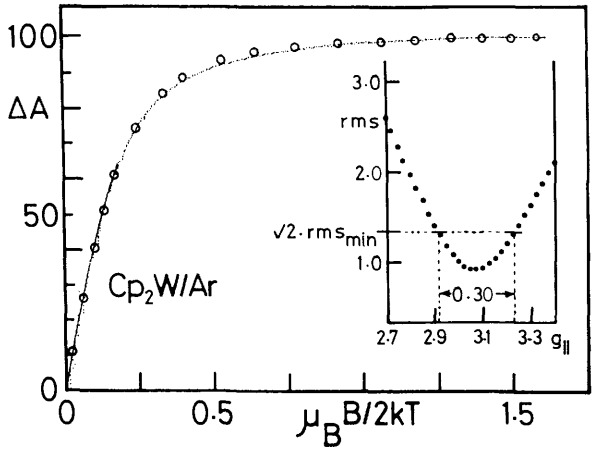

Figure 9 *Magnetization curve recorded* via *m.c.d. of* Cp_2W *in* Ar *at* 390 nm. *The experimental points are the fine dots plotted as normalized intensity* versus $\mu_B B/2kT$. *One set of experimental points is recorded at* 1.8 K *over the full abscissa range. Another set recorded at* 15 K *is superimposed over a narrower range up to* 0.25 $\mu_B B/2kT$. *The open circles show the best calculated points fitted to a selection of* 30 *experimental points. The inset shows the r.m.s. deviation of calculated from experimental points as a function of* $g_{\|}$ *value. The minimum gives the experimental* $g_{\|}$ *value of* 3.07 ± 0.15
(Reproduced with permission from Graham *et al.*, *J. Am. Chem. Soc.*, 1988, **110**, 7036, ref. 47)

B. Molybdenocene.[46,47,51]—The molybdenum compounds follow the pattern of metallocene generation, spectroscopy and reactivity established for their tungsten analogues with a few significant exceptions outlined below (Scheme 6). The i.r. spectrum of molybdenocene exhibits the pattern of broad and missing peaks associated with Jahn–Teller distorted chromocene rather than with ferrocene, and the electronic i.r. band is absent. Since the spin–orbit coupling constant for molybdenum is about four times smaller than for tungsten, we deduce that the Jahn–Teller distortion is no longer quenched by the spin–orbit effects. The m.c.d. experiments indicate that molybdenocene, like tungstenocene, is paramagnetic, but with a slightly reduced value of $g_{\|}$ (Table 1). The first u.v. absorption is moved about 1000 cm^{-1} to lower energy, bringing it into the right region for Kr^+ laser excitation. The l.i.f. spectrum enables us to measure the value of the symmetric (ring–metal–ring) stretching mode in the ground state (Figure 11, Table 2). Photolysis into the second charge-transfer band of Cp_2Mo at 312 nm causes reaction with CO to form Cp_2MoCO. Such photoinduced reaction with CO has also been demonstrated for Cp_2Cr and Cp_2V. The thermal back-reaction of Cp_2Mo with CO is observed at about 60 K only in the presence of 1% excess CO.

C. Rhenocene and Related Compounds.[25,47,52]—Photolysis of Cp_2ReH in argon

[51] P. Grebenik, A. J. Downs, M. L. H. Green, and R. N. Perutz, *J. Chem. Soc., Chem. Commun.*, 1979, 742; J. Chetwynd-Talbot, P. Grebenik, and R. N. Perutz, *Inorg. Chem.*, 1982, **21**, 3647.
[52] P.A.Cox, P. Grebenik, R. N. Perutz, R. G. Graham, and R. Grinter, *Chem. Phys. Lett.*, 1984, **108**, 415.

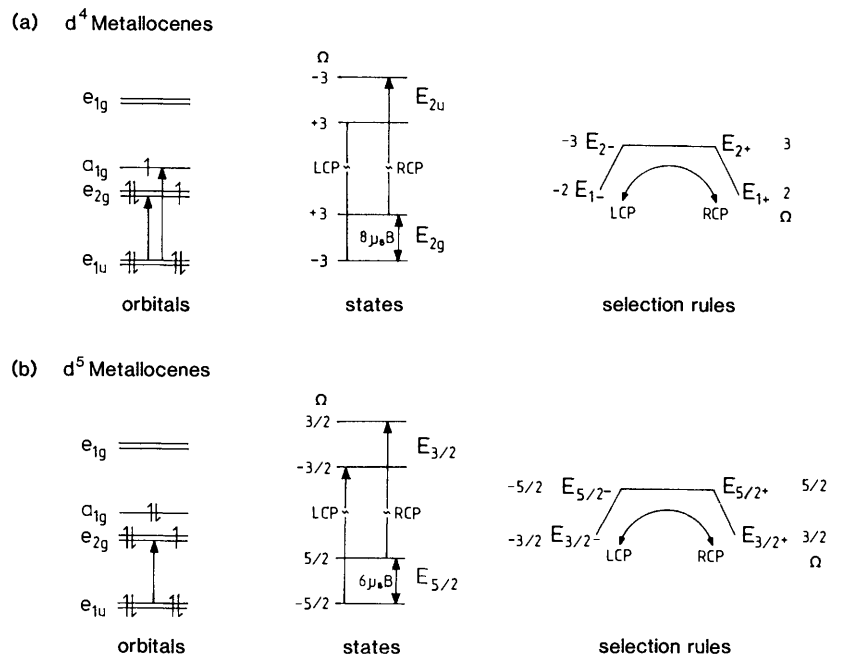

Figure 10 *Diagrams showing the basis of the u.v./vis absorptions and m.c.d. spectra of open-shell heavy metallocenes. (a) for a* d^4 *configuration, (b) for* d^5 *metallocenes. In each case the left-hand diagram shows the one-electron energy levels with allowed l.m.c.t. transitions. The* g *and* u *labels appropriate to* D_{5d} *symmetry are intended to emphasize that the c.t. transitions are allowed. The central diagram shows the many-electron states in a magnetic field with the allowed m.c.d. transitions, the total angular momentum* (Ω) *and the Zeeman splitting of the ground term in the ionic limit. The right-hand diagram shows how the different sub-states are linked by the m.c.d. selection rules. In such a cyclic system the angular momentum is usually raised/lowered by one unit, but it is also possible to move from,* e.g. $\Omega = 3$ *to* $\Omega = -3$, *a transition which could not occur in a linear molecule*

Table 1 g *values and lowest energy l.m.c.t. bands of* 16- *and* 17-*electron metallocenes*

Metallocene/ Matrix	$g_{\|}$ *(method)*		*l.m.c.t. (0,0) transition/* cm^{-1}
Cp_2Mo/Ar	2.75(18)	(m.c.d.)	23 987
Cp_2W/Ar	3.07(15)	(m.c.d.)	24 900
Cp_2Re/N_2	5.34(36)	(m.c.d.)	20 411
Cp^*_2Re/Ar	5.07(19)	(m.c.d.)	16 574
Cp^*_2Re/toluene	5.081(3)	(e.s.r.)	16 234
$[Cp^*_2Ru]^+$	2.059[a]	(e.s.r.)	20 000
$[Cp^*_2Os]^+[BF_4^-]/CD_2Cl_2$	5.27[b]	(e.s.r.)	—

[a] $g_\perp = 2.008$ ref. 68. [b] $g_\perp = 1.99$ ref. 67.

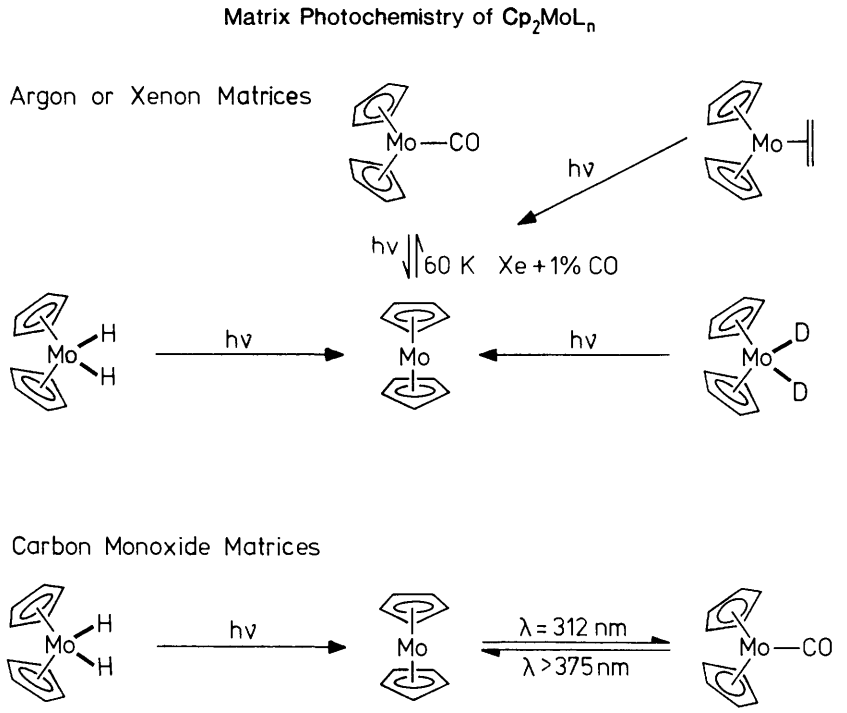

Scheme 6

Table 2 *Skeletal modes of metallocenes (in D_{5d} symmetry) and lowest energy l.m.c.t. electronic transitions, given as* (0,0) *transition where available* (ν/cm^{-1}). *Data for Ar matrices except where stated*

	$\nu'_4(a_{1g})$ *sym. stretch ground state*	$\nu'_4(a_{1g})$ *sym. stretch excited state*	$\nu_{16}(e_{1g})$ *sym. tilt*	$\nu_{11}(a_{2u})$ *antisym. stretch*	$\nu_{21}(e_{1u})$ *antisym. tilt*	*l.m.c.t.* (0,0)
Cp_2V	258[b]	—	331[b]	429	385	~33 900
Cp_2Cr	273[b]	—	370[b]	438	408[c]	~30 000
Cp_2Fe	303[a]	—	338[a]	478	492	—
Cp_2Mo	302	307	—	350	—	23 987
Cp_2Ru	330[a]	—	400[a]	387	458	—
Cp_2W	—	303	—	324	264	24 963
Cp_2Re	326	337	—	316	298	20 411
Cp_2Os	356[c]	—	415[c]	353[c]	428[c]	—

[a] Raman spectrum of solution from E. R. Lipincott and R. D. Nelson, *Spectrochim. Acta*, 1958, **10**, 307. [b] Raman spectrum of solid at 90 K from V. T. Aleksanyan, B. V. Lokshin, G. K. Borisov, G. G. Devyatykh, A. S. Smirnov, R. V. Nazarova, J. A. Koningstein, and B. F. Gächter, *J. Organomet. Chem.*, 1977, **124**, 293. [c] From B. V. Lokshin, V. T. Aleksanyan, and E. B. Rusach, *J. Organomet. Chem.*, 1975, **86**, 253.

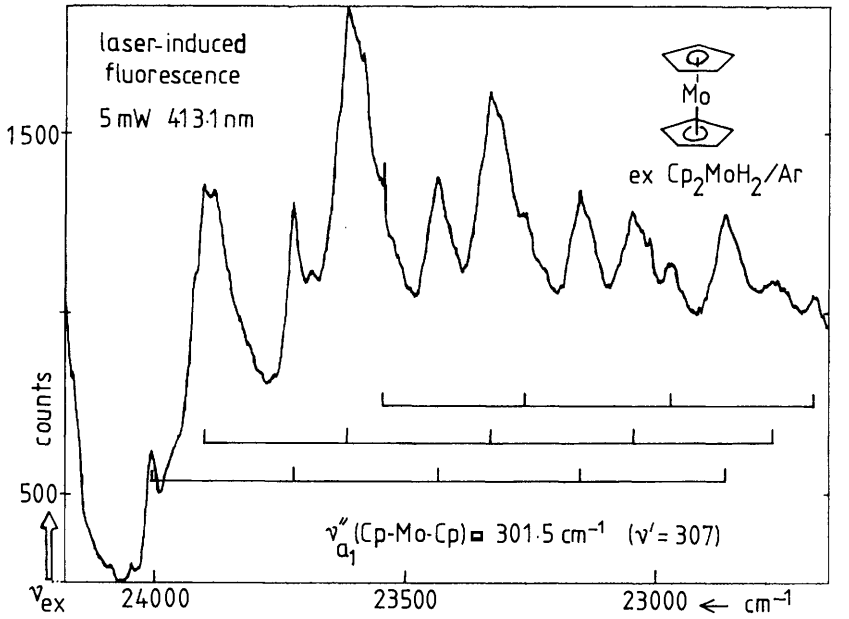

Figure 11 *Laser-induced fluorescence (l.i.f.) spectra of* Cp_2Mo *measured on an argon matrix following photolysis of* Cp_2MoH_2 *in Ar. The l.i.f. spectrum is excited by* 5mW *of* 413.1 nm *radiation from a* Kr^+ *laser. The band corresponds to an allowed l.m.c.t. transition with superimposed vibrational progression. The value of* ν_{sym} (ring–Mo–ring) *is significantly lower in the ground state than in the excited state*

matrices fails to cause reaction, but this compound is photosensitive in nitrogen, carbon monoxide, or CO/Ar (1:1) matrices. One of the photoproducts is common to all these matrices and exhibits i.r. spectra consistent with a metallocene. The assignment to rhenocene is supported by deuteriation at the hydridic position and on the rings, but the most decisive evidence comes from the visible spectrum, which exhibits a highly structured, intense transition with an onset close to 500 nm. Moreover, the l.i.f. spectrum obtained by irradiation into this band is even more highly resolved than the absorption spectrum (Figure 12a,c) proving that the molecule has a parallel ring structure. The hydrogen atoms expelled in this reaction are captured in the presence of CO to form the HCO radical. Evidently, they do not acquire enough translational energy to escape the cage in argon matrices, but manage to escape in nitrogen matrices. M.c.d. spectra prove the paramagnetism of Cp_2Re (Figure 12b) and the magnetization behaviour shows that it has a $^2E_2$ ($\Omega = 5/2$) ground state with a value of $g_{\|}$ reduced surprisingly little from the ionic limit of six (Table 1). The electronic structure is akin to that of tungstenocene, since the extra electron occupies an a_1 orbital. The visible band may be assigned unambiguously to a l.m.c.t. transition ($E_{5/2} \rightarrow E_{3/2}$) from the sign of the dichroism and the shift on permethylation (see

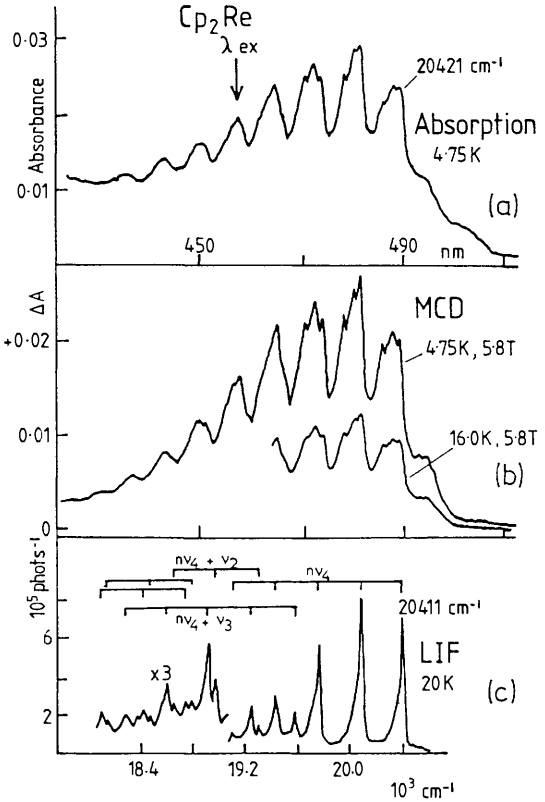

Figure 12 (*a*) *Visible absorption spectrum of* Cp_2Re *observed following u.v. photolysis of* Cp_2ReH *in a* N_2 *matrix; the arrow shows the excitation wavelength for fluorescence.* (*b*) *M.c.d. spectrum on the same sample as* (*a*) *at indicated temperatures and magnetic field.* (*c*) *L.i.f. spectrum of* Cp_2Re *excited at* 465.8 nm *showing progressions in* ν_4 (*ring–metal–ring symmetric stretch*) *and* ($\nu_4 + \nu_x$). *Notice change in scale direction from* (*a*)
(Reproduced with permission from Cox *et al., Chem. Phys. Lett.*, 1984, **108**, 415, ref. 52)

below). The l.i.f. spectrum allows precise location of the (0,0) transition and measurement of several vibrational modes forbidden in the i.r. It is dominated by progressions in the symmetric (ring–metal–ring) stretching mode (Table 2). Charge-transfer excitation causes an increase in the frequency of this mode from 326 to 337 cm^{-1} in accord with population of the bonding e_2 orbital. The l.i.f. spectrum in nitrogen matrices is consistent with complete vibrational relaxation in the upper state, but the question of vibrational relaxation in CO matrices is less certain, since there may be interference from HCO.

Loss of hydrogen atoms from Cp_2ReH is not the only photoprocess observed. In addition, we find that the molecule undergoes ligand attack by the CO or N_2 to form products of the type $Cp(\eta^3\text{-}C_5H_5)ReH(L)$. For L = CO this formulation

is supported by ^{2}H substitution of the hydride and ^{13}CO substitution, but we cannot prove by vibrational spectroscopy that the η^5–η^3 ring-slip occurs. Nevertheless, this formulation is strongly supported by comparison with Brintzinger's $Cp(\eta^3\text{-}C_5H_5)W(CO)_2$.[53a] For L = N_2 the addition product is shown to be a monodinitrogen complex by use of a $^{15}N_2/^{14}N_2$ (1:1) matrix. Prolonged photolysis in nitrogen matrices does not cause any additional reaction, but several further carbonyl products are observed in CO matrices. Two of them can be identified as $Cp(\eta^2\text{-}C_5H_6)Re(CO)_2$ and $CpRe(CO)_3$ by direct deposition of the stable compounds, as can expelled cyclopentadiene. This enables us to build up a very detailed picture of the reaction pathway (Scheme 7). Following the initial ring-slip and ligand attack, a second molecule of CO attacks inducing a second ring-slip. In the next stage, hydrogen migration occurs to form $Cp(\eta^2\text{-}C_5H_6)Re(CO)_2$. Finally C_5H_6 is expelled and another CO attacks to give $CpRe(CO)_3$. The use of the last two compounds as precursors allowed us to show that the sense of these reactions may be reversed in argon matrices. The role of ring-slip reactions has been reviewed recently,[53b] while ring-metal hydrogen migrations have been followed in other Re compounds by n.m.r.[27]

D. Cp_2MH and Cp_2MCO (M = Nb, Ta).[26]—Photolysis of Cp_2TaH_3 in Ar or N_2 matrices gives rise to a product exhibiting bands in the Ta–H stretching region. The same product, together with CO, may be accessed by photolysis of $Cp_2TaH(CO)$, allowing it to be identified as the 16-electron monohydride, Cp_2TaH. This complex exhibits a large number of absorptions in the mid-infrared and a broad u.v. spectrum, as expected for a bent sandwich complex. Like the isoelectronic Cp_2W, it may be a spin triplet, but the m.c.d. experiments are not yet conclusive. Photolysis of Cp_2TaH_3 in CO matrices causes efficient conversion into $Cp_2TaH(CO)$ followed by further carbonyl products on prolonged photolysis. When instead, $Cp_2TaH(CO)$ is deposited into a CO matrix directly and photolysed, the same photoproducts are formed. The first pair of products are identified as HCO and Cp_2TaCO, the products of homolysis of the Ta–H bond (Scheme 8). Traces of Cp_2TaCO are also generated in argon matrices. This 17-electron complex may be compared to the stable first-row analogue, Cp_2VCO. The behaviour of the niobium compounds is very similar to their tantalum analogues.

In spite of the recent suggestions of non-classical binding of hydrogen in Cp_2NbH_3,[29] the spectra of this molecule isolated in low-temperature matrices bear a close resemblance to those of its tantalum analogue. The ν(NbH) frequencies of Cp_2NbH_3 are shifted to low frequency by about 40 cm^{-1} relative to the tantalum compound, typical for a second-row/third-row pair. Moreover, ν(NbH) for Cp_2NbH_3, $Cp_2NbH(CO)$, and Cp_2NbH all lie very close to 1720 cm^{-1}, implying that Cp_2NbH_3 adopts the normal hydride structure in its ground state. We can also exclude photochemical isomerization to a non-classical complex, since the photoproduct from $Cp_2NbH(CO)$ has the same i.r. spectrum.

[53] (*a*) G. Huttner, H. H. Brintzinger, L. G. Bell, P. Friedrich, V. Bejenke, and D. Neugebauer, *J. Organomet. Chem.*, 1978, **145**, 329; (*b*) J. M. O'Connor and C. P. Casey, *Chem. Rev.*, 1987, **87**, 307.

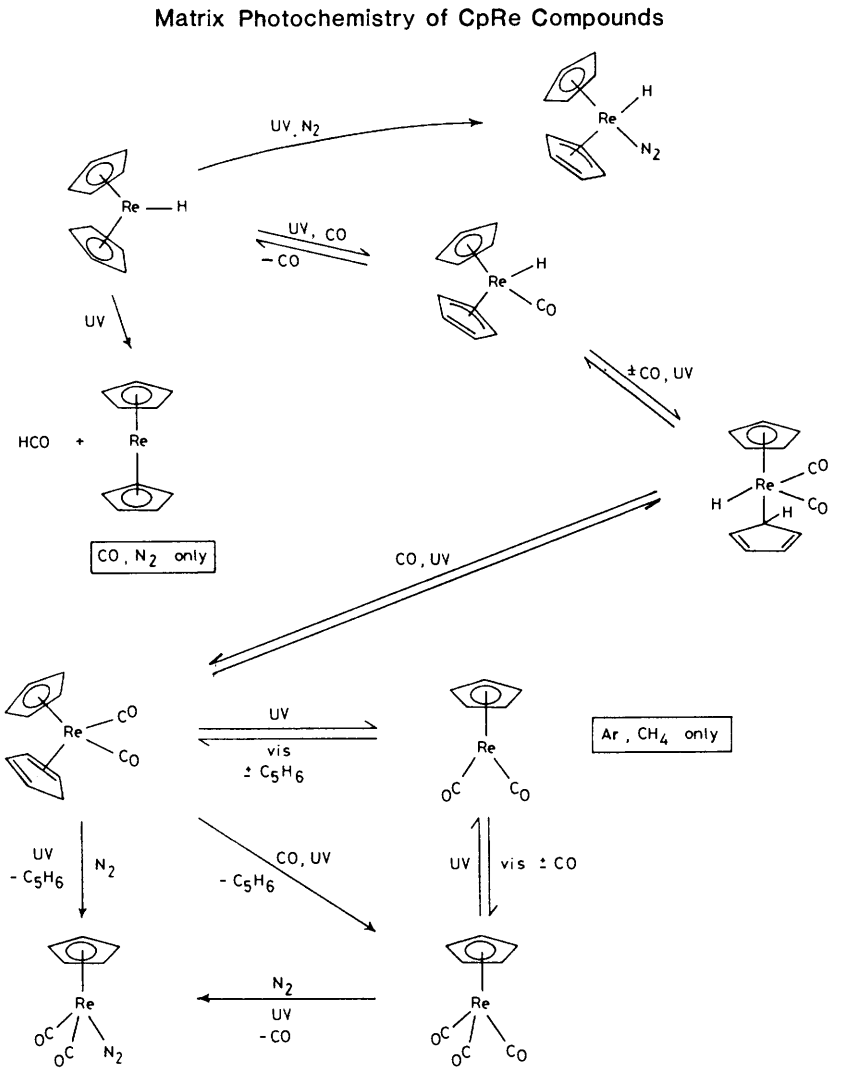

Scheme 7

(Reproduced with permission from Chetwynd-Talbot *et al.*, *Inorg. Chem.*, 1983, **22**, 1675, ref. 25)

One of the benefits of the studies of these and other Cp_2MH_n complexes has been an analysis of metal–hydrogen stretching frequencies, which prove to conform to a regular pattern given by the empirical equations:[54]

[54] R. B. Girling, P. Grebenik, and R. N. Perutz, *Inorg. Chem.*, 1986, **25**, 31.

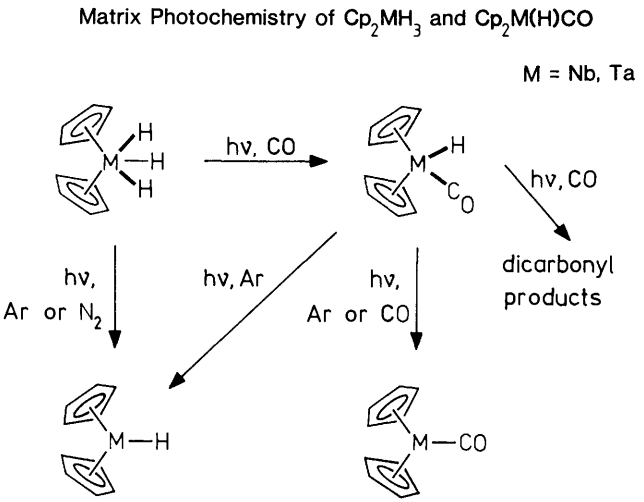

Scheme 8

(Reproduced with permission from Baynham *et al.*, *J. Organomet. Chem.*, 1985, **284**, 229, ref. 26)

Neutral $\nu(MH_n) = 1688 + 55\delta + 136(x - 5) + 15(y - 3)$ (7)

Cationic and Neutral $\nu(MH_n) = 1686 + 59\delta + 131(x - 5) + 20(y - 3) + 24z$ (8)

where $\delta = 0$ for $4d$ and $\delta = 1$ for $5d$ metals, x is the group of the periodic table to which the metal belongs, y is the oxidation state, and z the charge on the complex.

E. Photoprocesses in Matrices.—We are now in a position to collate the photoprocesses observed in the matrix reactions of bis(η^5-cyclopentadienyl) metal complexes. Of particular interest are those reactions available to metal hydrides (Scheme 9): (i) concerted elimination of H_2 and CH_3–H, (ii) homolysis of M–H bonds, and (iii) metal-to-ring migration. Other dissociative reactions include cleavage of metal alkene bonds (alkene = C_2H_4 or cyclo-C_5H_6), and the familiar cleavage of M–CO bonds. It is significant that the expulsion of CO is not necessarily the most efficient process. There is more in-cage recombination on photolysis of $Cp_2Ta(H)CO$ than of Cp_2TaH_3. The same is probably true of the $Cp_2WCO/Cp_2W(C_2H_4)$ pair. Associative photochemical processes are confined to the reactions with CO and N_2. Examples are given in equations 9 and 10.

$$Cp_2ReH + L \xrightarrow{h\nu, L} Cp(\eta^3\text{-}C_5H_5)Re(H)L \longrightarrow \ldots \quad (9)$$

$$Cp_2M + CO \xrightarrow{h\nu, CO} Cp_2MCO\ (M = V, Cr, Mo) \quad (10)$$

Primary Photoprocesses of Metal Hydrides in Matrices

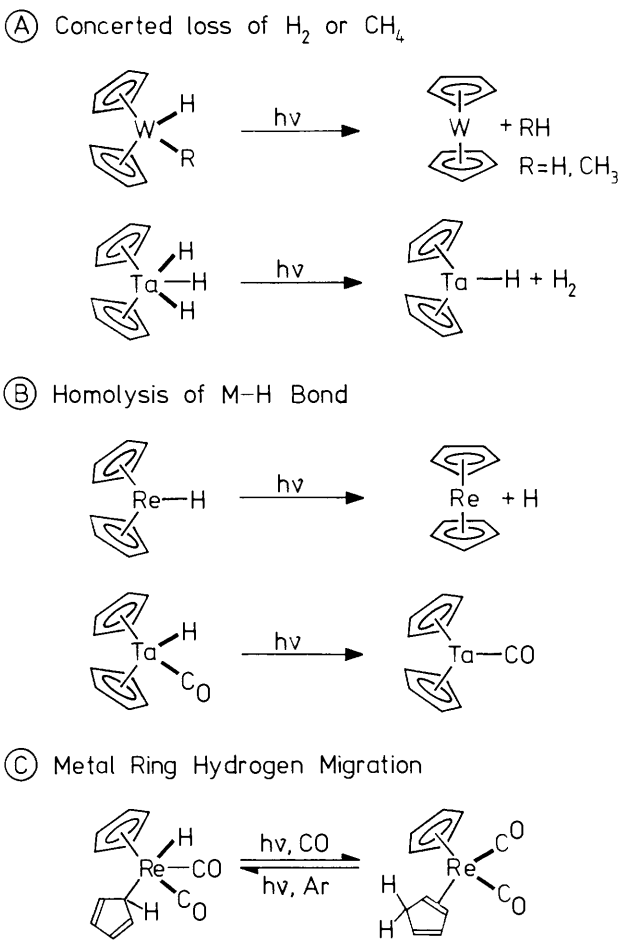

Scheme 9

The stepwise ring-slips of $(\eta^5\text{-}C_5H_5) \longrightarrow (\eta^3\text{-}C_5H_5) \longrightarrow (\eta^1\text{-}C_5H_5)$ are observed only as part of the associative reaction with CO or N_2.

These photoprocesses cover much of the overall range observed for organometallics.[55] When compared to the solution processes for metal alkyls[56]

[55] R. B. Hitam, K. A. Mahmoud, and A. J. Rest, *Coord. Chem. Rev.*, 1984, **55**, 1; R. N. Perutz in 'Chemistry and Physics of Matrix-Isolated Species', ed. L. Andrews and M. Moskovits, North-Holland, in press.

[56] H. G. Alt, *Angew. Chem., Int. Ed. Engl.*, 1984, **23**, 766.

and hydrides,[57] it is the homolytic reactions which are restricted in matrices. It is rare to observe M–H homolysis without the presence of CO to trap the hydrogen atoms. (Cp_2ReH in N_2 is an exception.) We have not succeeded in observing metal–alkyl homolysis at all. For instance, $Cp_2Zr(CH_3)_2$ is photoactive in solution but inert in argon or carbon monoxide matrices.

It is extremely difficult to trace the detailed photochemical pathways of Cp_2MH_n complexes, but some assistance is provided by state correlation diagrams which show that the reactions:

$$Cp_2MH_2 \longrightarrow Cp_2M + H_2 \qquad (11)$$

$$Cp_2MCO \longrightarrow Cp_2M + CO \quad (M = Mo, W) \qquad (12)$$

are thermally forbidden but photochemically allowed.[58] For example, low-lying $^3A_1$ and $^3B_2$ excited states of Cp_2MH_2 correlate with the ground state of Cp_2M (Figure 13). Population of the a_1* level favours concerted M–H bond cleavage and H–H bond formation. Although this argument identifies successfully those reactions which are photochemically allowed, the notion of thermally forbidden reactions is limited because of the high spin–orbit coupling constant of these metals. Thus triplet Cp_2M reacts with CO to form singlet Cp_2MCO even at 60 K. The matrix reaction of Cp_2Mo with CO proves to be slower than that of Cp_2W in keeping with the smaller spin–orbit coupling constant. Intersystem crossing rates are not known for compounds of these elements, but such rates have been measured for spin-equilibrium iron complexes in solution. Typical values for $S = 5/2 \rightleftharpoons S = 1/2$ i.s.c. rates fall in the range 10^5—10^9 s^{-1}, suggesting even faster rates for heavier transition elements.[59]

6 Direct Detection of Reactive Metallocenes in Solution

The matrix isolation experiments give some indication of the reactivity of molybdenocene and tungstenocene, but almost none for rhenocene. It should be possible to make use of the matrix u.v./vis spectra to identify transient metallocenes formed by flash photolysis. Laser flash photolysis of Cp_2MoH_2 does indeed generate a transient with an almost identical u.v. spectrum to matrix-isolated Cp_2Mo, and which decays in about 10^{-5} s (Figure 14).[60] These experiments show that Cp_2Mo does not dimerize, but decays *via* reaction with Cp_2MoH_2, to form a dinuclear intermediate which reacts further on a millisecond timescale to form the final product (Scheme 10). Other transients such as $Cr(CO)_5$[4] and $CpMn(CO)_2$[61] also decay by reaction with their parent molecules leading to the nickname Oedipus complexes! Molybdenocene is quenched by CO,

[57] G. L. Geoffroy, *Prog. Inorg. Chem.*, 1980, **27**, 123.
[58] A. Veillard, *Nouv. J. Chim.*, 1981, **5**, 599.
[59] R. A. Binstead, J. K. Beattie, T. G. Dewey, and D. H. Turner, *J. Am. Chem. Soc.*, 1980, **102**, 6447; E. V. Dose, M. A. Hoselton, N. Sutin, M. F. Tweedle, and L. J. Wilson, *ibid.*, 1980, **100**, 1141; C. L. Xie and D. N. Hendrickson, *ibid.*, 1987, **109**, 6981.
[60] R. N. Perutz and J. C. Scaiano, *J. Chem. Soc., Chem. Commun.*, 1984, 457.
[61] B. S. Creaven, A. J. Dixon, J. M. Kelly, C. Long, and M. Poliakoff, *Organometallics*, 1987, **6**, 2600.

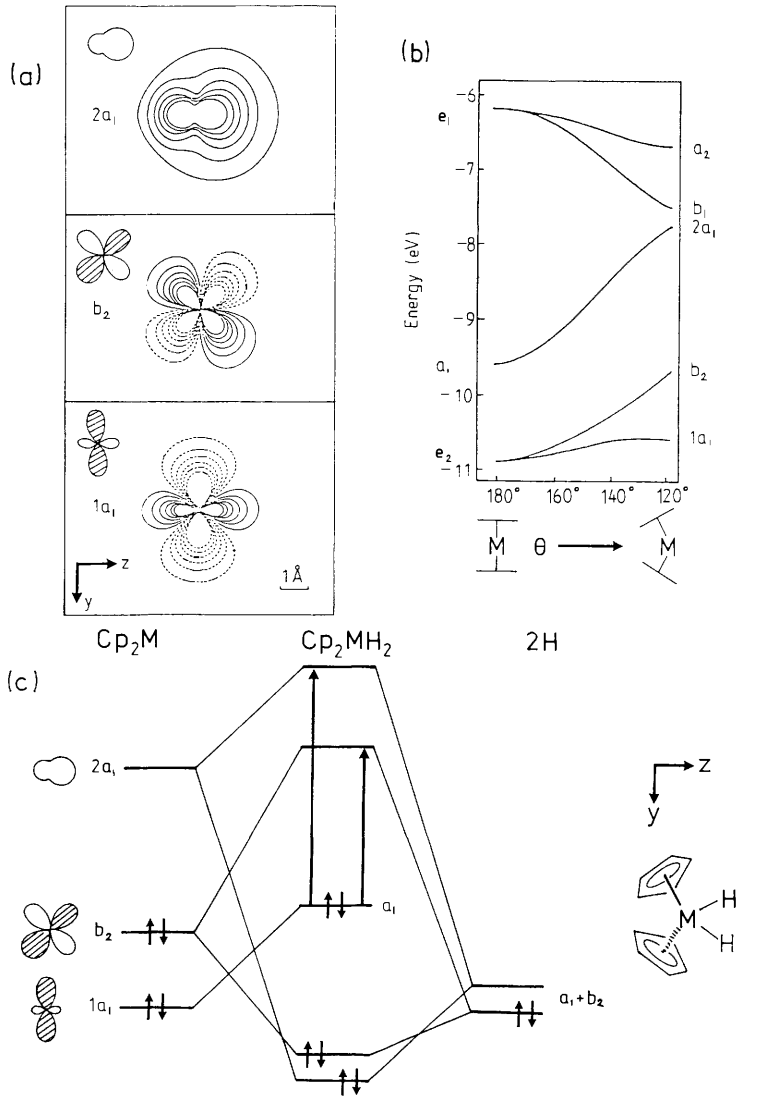

Figure 13 (*a*) *Contour diagram in the* yz *plane of the three frontier orbitals of a bent* Cp_2M *unit computed at a bending angle* $\theta = 136°$. *From top to bottom* $2a_1$, b_2, $1a_1$. *Solid line = positive, dashed line = negative contour of the wave function.* (*b*) *Walsh diagram showing the variation in energy of the* Cp_2M *orbitals as a function of the bending angle* θ. (*c*) *Interaction diagram showing the bonding of the two hydrogens to* Cp_2M *to form* Cp_2MH_2. *The orbitals of* Cp_2M *are shown as in* (*a*). *The arrows indicate allowed transitions which labilize the hydride ligands. The upper state should simultaneously make the* H–H *bond*
(Adapted with permission from Lauher and Hoffmann, *J. Am. Chem. Soc.*, 1976, **98**, 1729)

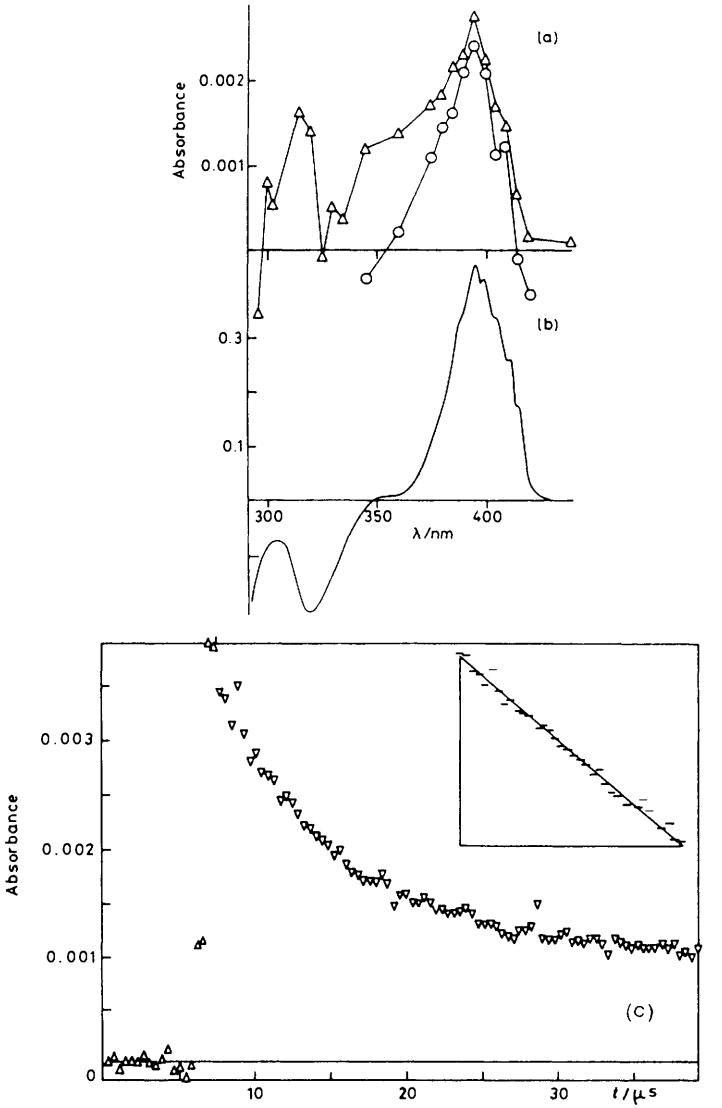

Figure 14 (*a*) *Difference spectrum generated by laser flash photolysis of* Cp_2MoH_2 *in thf at* 300 K. Δ *Average of data recorded in the first* 4μs *after the flash.* ○ *same but with residual absorption remaining after* 20μs *substracted.* (*b*) *Difference spectrum resulting from photolysis of* Cp_2MoH_2 *in* Ar *at* 20 K. *In both* (*a*) *and* (*b*) *positive absorptions are due to* Cp_2Mo *and negative absorptions due to* Cp_2MoH_2. (*c*) *Kinetic plot of the absorption of* Cp_2Mo *following laser flash photolysis of* Cp_2MoH_2 *in thf saturated with* CO, *monitored at* 395 nm. *The inset shows the first order plot giving a lifetime of* 7.8 μs
(Reproduced with permission from Perutz and Scaiano, *J. Chem. Soc., Chem. Commun.*, 1984, 457, ref. 60.)

Laser Flash Photolysis of Cp_2MoH_2

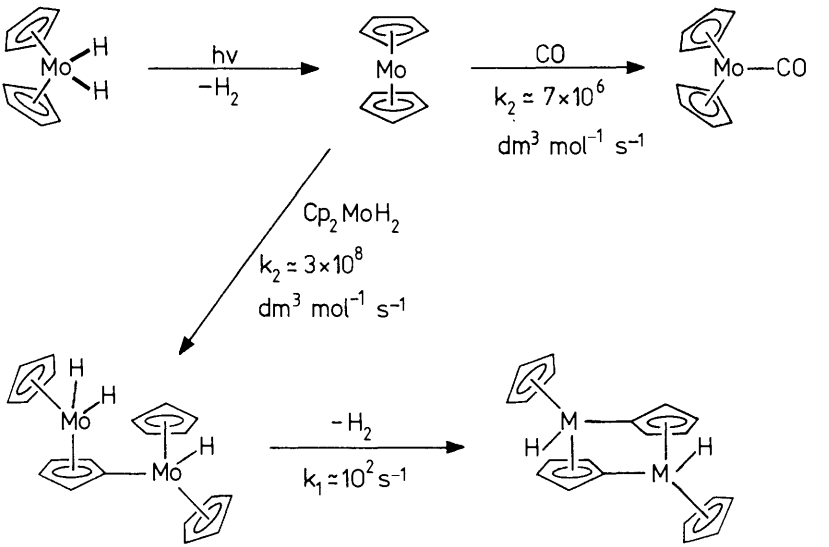

Scheme 10

but the rate constant for reaction with CO is appreciably lower than for reaction with Cp_2MoH_2, implying that ligand replacement reactions require a large excess of added ligand. The spectrum of Cp_2Mo and its reactivity are unaffected by a change of solvent from thf to cyclohexane. These experiments represent a dramatic demonstration of the complementarity of matrix isolation and flash photolysis studies. The chief limitation to any extension of the time-resolved experiments lies in the low quantum yields (see above). However, recent developments suggest that Cp_2WL complexes may have sufficiently high quantum yields to permit observation of tungstenocene.

7 Decamethylmetallocenes

Is it possible to overcome the instability of the d^4 and d^5 metallocenes with the aid of the pentamethylcyclopentadienyl (Cp*) ligand which is far bulkier and more strongly electron-donating? There are extensive studies of the decamethylmetallocenes of the first-row elements which illustrate the nature of the stereoelectronic differences between Cp and Cp* ligands. The steric effect is shown by the switch from an eclipsed (D_{5h}) structure for Cp_2Fe to a highly ordered, staggered (D_{5d}) structure for $Cp^*{}_2Fe$.[62] The electronic effect is apparent in the photoelectron spectra which show a shift to lower ionization energy in the

[62] D. P. Freyberg, J. L. Robbins, K. N. Raymond, and J. C. Smart, *J. Am. Chem. Soc.*, 1979, **101**, 892.

Synthesis and Solution Photochemistry of $Cp^*_2MH_n$

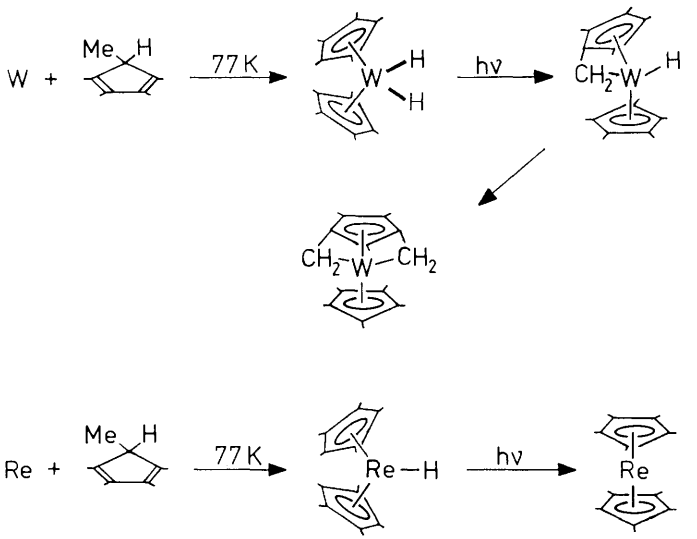

Scheme 11

d ionizations of 0.95 eV for a_1 and 0.88 eV for e_2 orbitals (averaged over data from several compounds).[37] An increase in the ligand-field splitting Δ_1 is demonstrated by the example of Cp^*_2Mn which is entirely low spin, $^2E_2$.[41] A detailed e.p.r. study of Cp^*_2Co and $[Cp^*_2Ni]^+$, however, fails to detect any change in covalency or ligand-field parameters compared to the unsubstituted analogues, but does point to a slight increase in the Jahn–Teller effect for the Cp* compounds.[63]

The hydrides $Cp^*_2WH_2$ and Cp^*_2ReH have been synthesized by co-condensation of C_5Me_5H with the metal vapour.[64,65] Solution photolysis of $Cp^*_2WH_2$ does not give the simple metallocene, but instead causes intramolecular oxidative addition of the ring methyl groups in two stages (Scheme 11),[64] so Cp^*_2W remains elusive. Stimulated by the matrix photochemistry of Cp_2ReH, Cloke and Day attempted photolysis of Cp^*_2ReH and demonstrated that it is converted into Cp^*_2Re which may be isolated in crystalline form (See Note in Proof). This complex has been examined in great detail by a variety of physical methods in vapour, crystal, solution, and matrix-isolate states.[49] The crystal structure shows that it adopts an eclipsed conformation like Cp^*_2Ru,[66] implying that steric

[63] L. Zoller, E. Moser, and J. H. Ammeter, *J. Phys. Chem.*, 1986, **90**, 6632.
[64] F. G. N. Cloke, J. C. Green, M. L. H. Green, and C. P. Morley, *J. Chem. Soc., Chem. Commun.*, 1985, 945.
[65] F. G. N. Cloke and J. P. Day, *J. Chem. Soc., Chem. Commun.*, 1985, 967.
[66] M. O. Albers, D. C. Liles, D. J. Robinson, A. Shaver, E. Singleton,, M. B. Wiege, J. C. A. Boeyens, and D. C. Levendis, *Organometallics*, 1986, **5**, 2321.

constraints are much smaller than in the first-row decamethylmetallocenes. Matrix-isolated Cp^*_2Re exhibits visible absorption and emission spectra which are very similar to those of rhenocene, but even more highly resolved. The m.c.d. measurements show that it adopts the same ground state, $E_{5/2}$, in the matrix. Notable features are as follows: (i) The value of $g_{\|}$ is reduced, probably because of increased covalency (Table 1). The value of $g_{\|}$ measured by m.c.d. magnetization in solid argon agrees almost exactly with that measured by e.p.r. in frozen toluene. A search up to very high field fails to reveal $g_{\perp}$, indicating that $g_{\perp} < 0.3$. (ii) The absorption and emission bands are red-shifted in accordance with a l.m.c.t. transition. (iii) The progression frequency observed in the electronic spectra is increased despite the mass effect of permethylation. This increase is associated with coupling between the symmetric (ring–metal–ring) stretching vibration and the symmetric deformation of the Cp* rings. A similar phenomenon has been observed for $[Cp^*_2Fe]^+$, but has been explained differently.[41] The similarity of the visible absorption spectra of Cp^*_2Re in toluene solution and in matrices and their lack of temperature dependence in solution imply that the electronic ground state is the same in both situations. However, changes are apparent in crystal and gas phases. The solid state magnetic moment conforms to the spin-only value and is essentially temperature independent, characteristics appropriate to a $^2A_1$ ground state. The gas-phase photoelectron spectra exhibit rich structure because of the open-shell configuration and high spin–orbit coupling constant. They are not explicable on the basis of the $E_{5/2}$ ground state established in matrices, but require an equilibrium between $E_{5/2}$ and $^2A_1$ states.

Very recently it has been demonstrated that salts of $[Cp^*_2Os]^+$ are also isolable.[67] The crystal structure of the BF_4^- salt shows a staggered structure which appears to be a consequence of steric hindrance introduced by a 0.5 Å compression of the inter-ring separation compared with Cp^*_2Re. The salts are e.p.r. silent except at very low temperature when signals at $g_{\|} = 5.27$, $g_{\perp} = 1.99$ are detected: strong evidence for an $E_{5/2}$ ground state like that of Cp^*_2Re. Magnetic susceptibility measurements on the solid and in solution prove that this state is maintained over a wide range of temperatures ($\mu_{eff} = 2.70\ \mu_B$). While the values of $g_{\|}$ are very similar for $[Cp^*_2Os]^+$, Cp^*_2Re, and Cp_2Re (Table 1), it is puzzling that $g_{\perp}$ should be close to 2 for $[Cp^*_2Os]^+$, but apparently too low to measure for the Re compounds. This result carries the implication that $[Cp^*_2Os]^+$ is far more distorted than the Re compounds. Electronic absorption spectra of $[Cp^*_2Os]^+$ are not yet available, but photoelectron spectra of Cp^*_2Os show that the $^2A_1$ state lies 0.35 eV above the ground $E_{5/2}$ state of the cation. Oxidation of $Cp_2{}^*Ru$ yields an unstable cation[68] with $g_{\|} = 2.059$ and $g_{\perp} = 2.008$ which decomposes readily to a tetramethylfulvene complex $[Cp^*Ru(\eta^6\text{-}C_5Me_4\text{-}exo\text{-}CH_2)]^+$ (*cf.* Scheme 11 and Note in Proof). The g values of $[Cp_2{}^*Ru]^+$ are intriguing since they are so different from the iron and the osmium complexes and do not correspond to the $^2A_1$ state either (then $g_{\|} = 2$, $g_{\perp} < 2$). The implication seems to be that the molecule is already drastically distorted.

[67] D. O'Hare, J. C. Green, T. P. Chadwick, and J. S. Miller, *Organometallics*, 1988, **7**, 1335.

Recent investigations of Cp^*_2Ta derivatives have led to the isolation of $Cp^*_2Ta(H)(CH_2)$,[69] a methylidene complex with no analogue in Cp_2Ta chemistry. This material reacts as if it were in equilibrium with $Cp^*_2TaCH_3$, forming $Cp^*_2Ta(CH_3)CO$ and $Cp^*_2Ta(CH_3)(CH_2)$ with CO and CH_2PMe_3 respectively. This behaviour is fully consistent with the 1,2-hydrogen shift chemistry associated with $[Cp_2WCH_3]^+$ as a *reaction intermediate*.[70] On current evidence, it seems unlikely that Cp^*_2TaH is stabilized by the Cp* rings,[71] but Cp^*_2TaCO might make a better target. (For comparison, the entire series of 16- and 17-electron compounds of vanadium Cp^*_2VH, $Cp^*_2VCH_3$ and Cp^*_2VCO are now known).[72]

8 Conclusions

Sixteen-electron metallocenes and their isoelectronic Cp_2MH analogues play a crucial role as reaction intermediates in photochemical and thermal reactions. The part played by 17-electron metallocenes Cp_2Re and $[Cp_2Os]^+$ remains more enigmatic, but recent experiments suggest that these molecules undergo rapid radical-type reactions to form dinuclear products. The molecular and electronic structure of the neutral 16- and 17-electron metallocenes have been elucidated by photochemical matrix isolation using a combination of spectroscopic methods. As a result we know considerably more about the structure of Cp_2W than of any other C–H activating organometallic intermediate. These metallocenes adopt a parallel ring structure with the same electron configurations as Cp_2Cr and $[Cp_2Fe]^+$. However, the Jahn–Teller effects which distort the first-row compounds are completely quenched by spin–orbit coupling for the third row compounds. Molybdenocene still exhibits signs of the Jahn–Teller effect. The electronic ground states, characterized in most detail by m.c.d. including magnetization measurements at very low temperature and high magnetic field, exhibit high values of $g_{\|}$. The high angular momentum is associated with the e_2 orbital (Table 1). The adoption of these states implies that Δ_2 remains small compared with electron repulsion, B, in contrast to the bis-arene metal complexes which adopt minimum angular momentum ground states even for the first-row elements ($^2A_1$ for 17-, $^1A_1$ for 16-electron complexes).[39] Unlike most organometallics, the metallocenes have very rich electronic absorption and emission spectra: they all exhibit a low-energy l.m.c.t. band (Table 1) as a result of their open-shell configuration. Like for $[Cp_2Fe]^+$,[41] this transition exhibits vibrational fine structure with progressions in ν_{sym} (ring–M–ring) which are brought out very effectively by the matrix isolation technique. Although some features of the electronic spectrum at higher energy are detected in absorption spectra, the sign information and the enhancement of the paramagnetic products

[68] U. Kölle and A. Salzer, *J. Organomet. Chem.*, 1983, **243**, C 27; U. Kölle and J. Grub, *ibid.*, 1985, **289**, 133.
[69] A. van Asselt, B. J. Burger, V. C. Gibson, and J. E. Bercaw, *J. Am. Chem. Soc.*, 1986, **108**
[70] J. C. Green, M. L. H. Green, and C. P. Morley, *Organometallics*, 1985, 7, 1303; G. A. Miller and N. J. Cooper, *J. Am. Chem. Soc.*, 1985, **107**, 709 and references therein.
[71] V. C. Gibson, J. E. Bercaw, W. J. Bruton, and R. D. Sanner, *Organometallics*, 1986, **5**, 977.
[72] C. J. Curtis, J. C. Smart, and J. L. Robbins, *Organometallics*, 1985, **4**, 1283.

makes m.c.d. spectra particularly powerful for finding these transitions. The skeletal vibrations of these metallocenes (Table 2) fall close to 300 cm^{-1}. The assignment of the i.r. bands to ν_{11} or ν_{21} is uncertain, but the symmetric (ring–metal–ring) stretching mode, ν_4, is unambiguous. This mode, which involves motion of the rings only, takes a similar or higher value for the unstable metallocenes compared to ferrocene. However, the values for the 18e metallocenes Cp_2Ru and Cp_2Os exceed those for the corresponding 16 and 17e complexes. Both for Cp_2Mo and Cp_2Re we observe an increase in ν_4 in the l.m.c.t. excited states.

The heavy metallocenes have a greatly enhanced reactivity which peaks in the third-row compounds with C–H activation processes, but quantitative kinetic measurements have barely begun. The most promising approach to quantifying reactivity, illustrated by the experiments on Cp_2Mo, makes use of the complementarity of matrix isolation and solution flash photolysis. This molecule proves to have a lifetime of about 10 μs in the presence of 0.03 mol dm^{-3} CO. Under preparative conditions with *ca.* 10^{-2} mol dm^{-3} Cp_2MoH_2, the pseudo first-order rate constant for reaction of Cp_2Mo with incoming ligand must exceed 3×10^6 s^{-1}, otherwise it will react with Cp_2MoH_2. The high reactivity of these molecules may be associated with increased overlap between metal and ligand typical of second- and third-row metals[73] (*cf.* also the M–H bond energies of Cp_2MoH_2 and Cp_2WH_2: 257 ± 8 and 311 ± 4 kJ mol^{-1} respectively).[74] It may also be dependent on the presence of a vacancy in the bonding e_2 orbital. Neither spin nor steric effects generate a significant barrier to reaction. In contrast, bis-arene complexes with a 17-electron configuration are stable, probably because the vacancy is in a non-bonding orbital.

The effect of changing from cyclopentadienyl to the pentamethylcyclopentadienyl ligand is to increase the steric bulk, but the electron density at the metal is increased simultaneously. The outcome in terms of reactivity is unexpected. The 16-electron decamethylmetallocenes are not detected, but appear to be unstable with respect to isomers formed by C–H insertion. The 17-electron decamethylmetallocenes Cp^*_2Re and $[Cp^*_2Os]^+$ are stable and isolable and have spectra and structures only marginally different from the corresponding metallocenes.

The experiments discussed in this review illustrate that a rich photochemistry is not confined to metal carbonyls, but is to be found among hydrido, alkyl, and alkene complexes. Recent developments, for instance in the photochemistry of CpRh and CpIr complexes[19,20,75] illustrate that those principles apply more generally. Meanwhile, the techniques of matrix isolation and laser flash photolysis, applied originally to metal carbonyl intermediates, have proved equally applicable

[73] P. Pyykkö, *Chem. Rev.*, 1988, **88**, 563; T. Ziegler, V. Tschinke, and A. Becke, *J. Am. Chem. Soc.*, 1987, **109**, 1351.

[74] J. C. Calada, A. R. Dias, J. A. Martinho-Simoes, M. A. V. Ribiero da Silva, *J. Organomet. Chem.*, 1979, **174**, 77; A. R. Dias and J. A. Martinho-Simoes, *Polyhedron*, in press.

[75] D. M. Haddleton, A. McCamley, and R. N. Perutz, *J. Am. Chem. Soc.*, 1988, **110**, 1809; D. M. Haddleton and R. N. Perutz, *J. Chem. Soc., Chem. Commun.*, 1986, 1734.

to other organometallics and form a powerful combination for the direct detection of reaction intermediates.

Acknowledgements.—Much of the success of the project to matrix isolate unstable metallocenes, now ten years old, can be attributed to the inspiration, skill, generosity, and forbearance of several of our colleagues. Dr Geoffrey Cloke, Dr Tony Cox, Dr Tony Downs, Dr Robin Graham, Dr Jennifer Green, Professor Malcolm Green, and Dr David Stern each played a major role.

Note Added in Proof. A by-product of the reaction of Re vapour and C_5Me_5H is $Cp^*Re(\eta^6\text{-}C_5Me_4\text{-}exo\text{-}CH_2)$. This compound is also formed on extended photolysis of Cp^*_2Re. Thus C–H insertion is observed for Cp^*_2Re as for the tungsten complex (Scheme 11) and the ruthenium cation, but not so rapidly as to prevent isolation of decamethylrhenocene (F. G. N. Cloke and J. P. Day, personal communication).